

Multiparton pp and pA collisions – from geometry to parton– parton correlations†

B. Blok¹, M. Strikman²

¹ Department of Physics, Technion – Israel Institute of Technology, Haifa, Israel

²Physics Department, Pennsylvania State University, University Park, USA

We derive expressions for the cross section of the multiparton interactions based on the analysis of the relevant Feynman diagrams. We express the cross sections through the double (triple, ...) generalized parton distributions (GPDs). In the mean field approximation for the double GPDs the answer is expressed through the integral over two gluon form factor which was measured in the exclusive DIS vector meson production. We explain under what conditions the derived expressions correspond to an intuitive picture of hard interactions in the impact parameter representation. The mean field approximation in which correlations of the partons are neglected fail to explain the data, while pQCD induced correlation enhance large p_{\perp} and $0.001 < x < 0.1$ typically enhance the cross section by a factor of 1.5 – 2 explaining the current data. We argue that in the small x kinematics ($10^{-4} \leq x \leq 10^{-3}$) where effects of perturbative correlations diminish, the nonperturbative mechanism kicks in and generates positive correlations comparable in magnitude with the perturbative ones. We explain how our technique can be used for calculations of MPI in the proton - nucleus scattering. The interplay of hard interactions and underlying event is discussed, as well as different geometric pictures for each of MPI mechanisms-pQCD, nonperturbative correlations and mean field. Predictions for value of σ_{eff} for various processes and a wide range of kinematics are given. We show that together different MPI mechanisms give good description of experimental data, both at Tevatron, and LHC, including the central kinematics studied by ATLAS and CMS detectors, and forward (heavy flavors) kinematics studied by LHCb.

† To be published in "Multiple parton Interactions at the LHC", P. Bartalini and J. Gaunt eds, World Scientific

PACS numbers: 12.38.-t, 13.85.-t, 13.85.Dz, 14.80.Bn

Keywords:

I. INTRODUCTION

It is widely realized now that hard *Multiple Parton Interactions* (MPI) occur with a probability of the order one in typical inelastic LHC proton-proton pp collisions. Indeed the ratio of the integral of the inclusive jet cross section with transverse momenta $p_{\perp} \geq \text{few GeV}$ and $\sigma_{inel}(NN)$ gives the average multiplicity of hard collisions (dijet production) larger than one, see e.g. [1, 2]. Hence MPI play an important role in the description of inelastic pp collisions. MPI were first introduced in the eighties [3, 4] and in the last decade became a subject of a number of the theoretical studies, see e.g. [5–28] and references therein.

Also, in the past several years a number of Double Parton Scattering (DPS) measurements in different channels were carried out [29–39], while many Monte Carlo (MC) event generators now incorporate MPIs [40–50].

The double parton scattering (DPS) cross section is traditionally parameterized as

$$\frac{d\sigma(4 \rightarrow 4)}{d\Omega_1 d\Omega_2} = \frac{1}{\sigma_{eff}} \frac{d\sigma(2 \rightarrow 2)}{d\Omega_1} \frac{d\sigma(2 \rightarrow 2)}{d\Omega_2}, \quad (1)$$

where Ω_i is the phase volume for production of a pair of jets where σ_{eff} is a priori a function of x_i, p_{t_i} . Initially it was conjectured [3] that parameter σ_{eff} is related to the total inelastic cross section of the hadron - hadron interactions.

Later on within the framework of the geometric picture implemented in the Monte Carlo models σ_{eff} was written as a convolution of the four single parton impact parameter distributions, $g(\rho_i)$ assuming that these distributions do not depend on x and on flavor, cf. Fig. 1.

$$\frac{1}{\sigma_{eff}} = \int d^2\rho_i d^2b g(\rho_1)g(\rho_3)g(\rho_2)g(\rho_3)g(\rho_4)\delta(\vec{\rho}_1 - \vec{\rho}_3 - \vec{b})\delta(\vec{\rho}_2 - \vec{\rho}_4 - \vec{b}). \quad (2)$$

One can see from Eq.2 that the factor σ_{eff} characterizes the transverse area occupied by the partons participating in two hard collisions. It also includes effect of possible longitudinal correlations between the partons.

Parameters of this distribution were chosen to reproduce the MPI data obtained at the Tevatron which reported $\sigma_{eff} \approx 15$ mb.

Further study used the QCD factorization theorem for the exclusive vector meson production to extract $g(\rho, x|Q^2)$ from the photo/electro production data. Under assumption that partons in colliding nucleons are not correlated a much larger $\sigma_{eff} \geq 30$ mb was found [51]. This strongly suggested that significant parton - parton correlations are present in nucleons.

In this paper we will summarize our studies of the mechanisms which generate perturbative and nonperturbative correlations between the partons and allow to explain many features of the

data. In particular we explain the geometry of MPI and show that the MPI cross section is given by the sum of the mean field contribution, pQCD and nonperturbative mechanisms, connected with nonfactorizable initial conditions. Each of these three mechanisms corresponds to its different range of impact parameters, (with the mean field one being most central). Together they lead to a good agreement of experimental MPI cross sections.

The text is organized as following.

In sec. 2 we present the geometrical picture of MPI and explain that hard collisions, in average correspond to much smaller impact parameters than the minimum bias inelastic collisions. In sec. 3 we review the parton level calculation of the DPS using Feynman diagram analysis which allows to express the DPS cross section through the convolution of two double generalized parton distributions (GPD). The double GPDs in the mean field approximation are expressed through a product of single GPDs which are extracted from the studies of the exclusive vector meson production. In section 4 we analyze contribution to the DPS of the correlation mechanism induced by the pQCD evolution. General expressions are derived both for the cross section differential in jet imbalances δ_{ij} and the cross section integrated over δ_{ij} .

The numerical results for the contribution of pQCD correlation mechanism are presented in sec. 5. We find that perturbative mechanism may enhance the DPS rates at large p_{\perp} (large virtualities) and $x \sim 10^{-2} \div 10^{-3}$ by a factor 1.5 – 2 allowing to explain the observed rates for a number of DPS processes.

In section 6 we argue that a new soft mechanism of the parton - parton correlations becomes important for $x \leq 10^{-3}$ which is due to presence of multiPomeron exchanges. We explain that this mechanism is relevant for the understanding of the rate of minijet production and as well as the production of two D-mesons in the forward kinematics studied by LHCb [36–39]. In section 7 we apply our technique to calculate the rate of MPI in proton - nucleus collisions taking into account pQCD corrections to the parton model approximation [24] and finding that pQCD corrections further increase the ratio of MPI in pp and pA scattering [25].

In section 8 we consider several consequences of the different impact parameter localization of the minimum bias and hard collisions. In particular we explain that b-space unitarity leads to requirement that jet production cross section should be suppressed was compared to the pQCD result even at large impact parameters.

Our conclusions are presented in section 9.

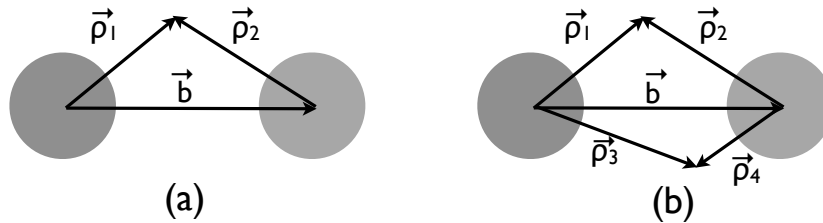


FIG. 1: Geometry of one and two hard collisions in impact parameter picture.

II. TRANSVERSE PICTURE OF MULTIPARTON INTERACTIONS

A. Impact parameter distribution in hard collisions

A natural framework for visualization of the MPI is the impact parameter representation of the collision. Indeed, in the high energy limit the angular momentum conservation implies that the impact parameter b becomes a good quantum number. Also the hard collisions are localized in the transverse plane at the relative distances $\sim 1/Q$ where Q is transverse momentum transfer. Combined, they lead to an intuitive picture of the MPI.

To describe the transverse geometry of the pp collisions with production of a dijet it is convenient to consider probability to find a parton with given x and transverse distance $\vec{\rho}$ from the nucleon transverse center of mass, $f_i(x_i, \vec{\rho}_i)$. This quantity allows a formal operator definition, and it is referred to as the diagonal generalized parton distribution (GPD). It is related to non-diagonal GPDs which enter in the description of the exclusive meson production (see Appendix for discussion of the information on ρ dependence of GPDs which is available from the studies of the exclusive vector meson production in the DIS.).

The inclusive cross section in the LT pQCD regime does not depend on the transverse structure of the colliding hadrons - the cross section is expressed through the convolution of parton densities. Indeed, we can write

$$\begin{aligned} \sigma_h &\propto \int d^2b d^2\rho_1 d^2\rho_2 \delta(\rho_1 + b - \rho_2) f_1(x_1, \rho_1) f_2(x_2, \rho_2) \sigma_{2 \rightarrow 2} = \\ &\int d^2b d^2\rho_1 d^2\rho_2 f_1(x_1, \rho_1) f_2(x_2, \rho_2) \sigma_{2 \rightarrow 2} = f_1(x_1) f_2(x_2) \sigma_{2 \rightarrow 2}. \end{aligned} \quad (3)$$

Here at the last step we used the relation between diagonal GPD and PDF: $\int d^2\rho f_j(x, \rho, Q^2) = f_j(x, Q^2)$.

At the same time, as soon as one wants to describe the structure of the final state in production

of say dijets, it is important to know whether a hard process occurs at different average impact parameters than in the minimum bias interactions. It turns out that at the LHC energies a dijet trigger selects, in average, a factor of two smaller impact parameters than in the minimum bias events. This implies that the multijet activity, energy flow should be much stronger in these events than in the minimum bias events. Obviously, the magnitude of the enhancement does depend on the transverse distribution of partons and on the correlation between the partons in the transverse plane. This information becomes available now. It is summarized in the Appendix.

In the case of collisions with N hard subprocesses the interaction picture corresponds to a pairwise localization of N partons of each of the nucleons at short distances (Fig. 1b), leading to the cross section of collision of hadrons a and b proportional to

$$\sigma_h^{(N)} \propto \int d^2b \prod_{i=1}^{i=N} d\rho_i d\rho'_i \delta(\rho_i + b - \rho'_i) f_a(\rho_i, Q_i) f_b(\rho'_i, Q_i). \quad (4)$$

The geometric pairwise overlap with N partons of hadrons a and b nearby pairwise provides a geometric factor L^{N-1} in the cross section for N hard collisions, where L is the linear scale proportional to the transverse linear scale of the colliding hadrons. Eq. 4 includes correlations between partons both on the hadronic distance scale and local correlations due to the QCD evolution. In the case of perturbative correlations when two partons of one of the colliding nucleons are close together the overlap factor is enhanced as compared to the uncorrelated case, see discussion in sec. 3.

Using the information on the transverse spatial distribution of partons in the nucleon, one can obtain the distribution over impact parameters in pp collisions with hard parton-parton processes [51]. It is given by the overlap of two parton wave functions as depicted in Fig. 1.

The probability distribution of pp impact parameters in events with a given hard process, $P_2(x_1, x_2, b|Q^2)$, is given by the ratio of the cross section at given b and the cross section integrated over b . As a result

$$P_2(x_1, x_2, b|Q^2) \equiv \int d^2\rho_1 \int d^2\rho_2 \delta^{(2)}(\mathbf{b} - \boldsymbol{\rho}_1 + \boldsymbol{\rho}_2) \times F_{2g}(x_1, \rho_1|Q^2) F_{2g}(x_2, \rho_2|Q^2), \quad (5)$$

which obviously satisfies the normalization condition

$$\int d^2b P_2(x_1, x_2, b|Q^2) = 1. \quad (6)$$

This distribution represents an essential tool for phenomenological studies of the underlying event in pp collisions [51, 52], see discussion in Sec. 7.

For the two parametrizations of Eq. (55), Eq. (5) leads to (for $x \equiv x_1 = x_2$)

$$P_2(x, b|Q^2) = \begin{cases} (4\pi B_g)^{-1} \exp[-b^2/(4B_g)], \\ [m_g^2/(12\pi)] (m_g b/2)^3 K_3(m_g b), \end{cases} \quad (7)$$

where the parameters B_g and m_g are taken at the appropriate values of x and Q^2 . Since B_g increases with a decrease of x , distribution over b depends on x 's of the colliding partons and their virtualities, however this effect is pretty small for production of jets at central rapidities, see e.g. Figs. 4, 5 in [52].

Comment A word of caution is necessary here. The transverse distance b for dijet events is defined as the distance between the transverse centers of mass of two nucleons. It may not coincide with b defined for soft interactions where soft partons play an important role. For example, if we consider dijet production due to the interaction of two partons with $x \sim 1$, $\rho_1, \rho_2 \sim 0$ since the transverse center of mass coincides with transverse position of the leading quark in the $x \rightarrow 1$ limit. As a result, b for the hard collision will be close to zero. On the other hand the rest of the partons may interact in this case at th every different transverse coordinates. As a result, such configurations may contribute to the inelastic pp cross section at much larger b for the soft interactions. However for the parton collisions at $x_1, x_2 \ll 1$ the recoil effects are small and so two values of b should be close.

B. Impact parameter distribution in minimum bias collisions

The derived distribution should be compared to the distribution of the minimum bias inelastic collisions which could be expressed through $\Gamma(s, b)$ that is the profile function of the pp elastic amplitude ($\Gamma(s, b) = 1$ if the interaction is completely absorptive at given b)

$$P_{\text{in}}(s, b) = [1 - |1 - \Gamma(s, b)|^2] / \sigma_{\text{in}}(s), \quad (8)$$

where $\int d^2b P_{\text{in}}(s, b) = 1$.

Our numerical studies indicate that the impact parameter distributions with the jet trigger (Eq.7) are much more narrow than that in minimum bias inelastic events at the same energy (Eq.8) – see Fig. 2, and that b -distribution for events with a dijet trigger is a very weak function of the p_T of the jets or their rapidities. For example, for the case of the pp collisions at $\sqrt{s} = 13$ GeV the median value of b , $b_{\text{median}} \approx 1.2$ fm and $b_{\text{median}} \approx 0.65$ fm for minimum bias and dijet trigger events[52].

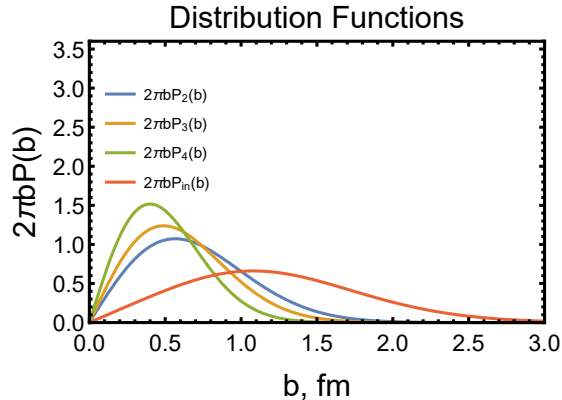


FIG. 2: Normalized probabilities of minimum bias, inclusive two, and four parton collisions and collision involving three partons as a function of the impact parameter.

Note here that in many experimental analyses the minimum bias cross section is defined as the inelastic nondiffractive cross section. Since inelastic diffraction is a peripheral process in pp scattering, $\sigma_{min.bias}$ defined this way corresponds to somewhat smaller b than the ones given by Eq. 8.

For $N \geq 2$ dijet processes

$$b_{median}(N) \approx \frac{1}{\sqrt{N}} b_{median}(N = 1). \quad (9)$$

Hence inclusive $N \geq 2$ processes are dominated by collisions at very small impact parameters where gluon fields of two nucleons strongly overlap: $b_{median} < 2r_g^{(N)}(x)$ (here $r_g^{(N)}(x) \geq 0.4 fm$ is the transverse radius of the gluon distribution in nucleons), cf. Fig. 2.

Since the large impact parameters give the dominant contribution to σ_{inel} our analysis indicates that there are two pretty distinctive classes of pp collisions - large b collisions which are predominantly soft and and central collisions with strongly enhanced rate of hard collisions. We refer to this pattern as the two transverse scale picture of pp collisions at collider energies [51].

III. GPD AND MEAN FIELD APPROACH TO MPI.

Description of the MPI is a multi-scale problem. This is not only because the separate parton-parton interactions may differ in hardness. More importantly, *each* single hard interaction possesses *two* very different hardness scales. The distinctive feature of the DPS is that it produces two pairs of nearly back-to-back jets, so that in the collision of partons 1 and 3 the first (larger) scale is given by the invariant mass of the jet pair, $Q^2 = 4J_{1\perp}^2 \simeq 4J_{3\perp}^2$, while the second scale is the magnitude

of the *total transverse momentum* of the pair: $\delta^2 = \delta_{13}^2$. It is important to stress that in the MPI physics there is *no factorization* in the usual sense of the word. The cross sections do not factorize into the product of the hard parton interaction cross sections and the multi-parton distributions depending on momentum fractions x_i and the hard scale(s). A general approach to double (multi) hard interactions has been developed in [6]. It turned out that the *transverse momentum* of the parton in the w.f. and that of its counterpart in the conjugated w.f. are indeed necessarily different, with their difference $\vec{\Delta}$ being conjugate to the relative transverse distance between the two partons in the hadron. This has led to introduction of the new object – *generalized double parton distribution*, ${}_2\text{GPD}$, which depends on a new momentum parameter $\vec{\Delta}$ [6, 9].

A. Generalized two-parton distribution

1. ${}_2\text{GPD}$ and their connection to wave functions.

In [6, 9] we have shown that the QFT description of the double hard parton collisions calls for introduction of ${}_2\text{GPD}$. Defined in the momentum space, it characterizes two-parton correlations inside hadron [6]: $D_h(x_1, x_2, Q_1^2, Q_2^2; \vec{\Delta})$. Here the index h refers to the hadron, x_1 and x_2 are the light-cone fractions of the parton momenta, and Q_1^2, Q_2^2 the corresponding hard scales. As has been mention above, the two-dimensional vector $\vec{\Delta}$ is the Fourier conjugate to the relative distance between the partons 1 and 2 in the impact parameter plane. The distribution obviously depends on the parton species; we suppress the corresponding indices for brevity.

The ${}_2\text{GPD}$ are expressed through multiparton light cone wave functions as:

$$\begin{aligned}
D(x_1, x_2, p_1^2, p_2^2, \vec{\Delta}) &= \sum_{n=3}^{\infty} \int \frac{d^2 k_1}{(2\pi)^2} \frac{d^2 k_2}{(2\pi)^2} \theta(p_1^2 - k_1^2) \theta(p_2^2 - k_2^2) \\
&\times \int \prod_{i \neq 1,2} \frac{d^2 k_i}{(2\pi)^2} \int_0^1 \prod_{i \neq 1,2} dx_i (2\pi)^3 \delta\left(\sum_{i=1}^{i=n} x_i - 1\right) \delta\left(\sum_{i=1}^{i=n} \vec{k}_i\right) \\
&\times \psi_n(x_1, \vec{k}_1, x_2, \vec{k}_2, \dots, \vec{k}_i, x_i, \dots) \psi_n^+(x_1, \vec{k}_1 + \vec{\Delta}, x_2, \vec{k}_2 - \vec{\Delta}, x_3, \vec{k}_3, \dots). \tag{10}
\end{aligned}$$

Note that this distribution is diagonal in the space of all partons except the two partons involved in the collision. Here ψ is the parton wave function normalized to one in the usual way. An appropriate summation over color and Lorentz indices is implied.

The double hard interaction cross section (and, in particular, that of production of two dijets) can be expressed through the convolution of ${}_2\text{GPD}$ s.

The *effective interaction area* σ_{eff} defined in Eq. 1 is given by the convolution of the ${}_2\text{GPDs}$ of incident hadrons over the transverse momentum parameter $\vec{\Delta}$ normalized by the product of single-parton inclusive pdfs:

$$\frac{1}{\sigma_{\text{eff}}} \equiv \frac{\int \frac{d^2\vec{\Delta}}{(2\pi)^2} D_{h_1}(x_1, x_2, Q_1^2, Q_2^2; \vec{\Delta}) D_{h_2}(x_3, x_4, Q_1^2, Q_2^2; -\vec{\Delta})}{D_{h_1}(x_1, Q_1^2) D_{h_1}(x_2, Q_2^2) D_{h_2}(x_3, Q_1^2) D_{h_2}(x_4, Q_2^2)}. \quad (11)$$

Eq. 11 (and similar expression for any number of MPI) can be rewritten in transverse coordinate representation and corresponds to the transverse geometry depicted in Fig. 1 with $\vec{\Delta}$ Fourier conjugated to the difference of transverse coordinates of partons: $\vec{\rho}_1 - \vec{\rho}_3$.

${}_2\text{GPDs}$ enter also the expressions for the differential distributions in the jet transverse momentum imbalances $\vec{\delta}_{ik}$ (integral of which over $\vec{\delta}_{ik}$ is the “total” DPS cross section – Eq.11. In the inclusive case the hardness parameters of the ${}_2\text{GPDs}$ are given by the jet transverse momenta Q_i^2 , while for the differential distributions — by the jet imbalances δ_{ik}^2 . The corresponding formulae derived in the leading collinear approximation of pQCD can be found in Ref. [9]. It is worth emphasizing here that the DPS cross section *does not factorize* into the product of the hard parton interaction cross sections and the two two-parton distributions depending on momentum fractions x_i and the hard scales, Q_1^2, Q_2^2 .

Note that one can introduce in the same way the N -particle GPD, G_N , which can be probed in the production of N pairs of jets [6]. In this case the first N arguments k_i are shifted by $\vec{\Delta}_i$ subject to the constraint $\sum_i \vec{\Delta}_i = 0$. So the cross section is proportional to

$$\begin{aligned} \sigma_{2N} \propto & \int \prod_{i=1}^{i=N} \frac{d\vec{\Delta}_i}{(2\pi)^2} D_a(x_1, \dots, x_N, \vec{\Delta}_1, \dots, \vec{\Delta}_N) \\ & \times D_b(x'_1, \dots, x'_N, \vec{\Delta}_1, \dots, \vec{\Delta}_N) \delta\left(\sum_{i=1}^{i=N} \vec{\Delta}_i\right). \end{aligned} \quad (12)$$

N -parton GPD are expressed through multiparton wave functions analogously to Eq.10.

The above approach allows to take into account consistently the perturbative mechanism of two-parton correlation when the two partons emerge from *perturbative splitting* of one parton taken from the hadron wave function since one needs to separate these correlations from the $2 \rightarrow 4$ mechanism of jet production.

In perturbative scenario the production of the parton pairs is concentrated at much smaller transverse distances between partons. As a result, the corresponding contribution to ${}_2\text{GPD}$. turns out to be practically independent of Δ^2 in a broad range, up to the hard scale(s) characterizing the hard process under consideration (Δ^2 only affects the lower limit of the transverse momentum

integrals in the parton cascades, resulting in a mild logarithmic dependence). The weak dependence on Δ results in a distribution over impact parameters for DPS which is intermediate between the mean field contribution and dijet b - distributions, cf. Fig. 2. Given essentially different dependence

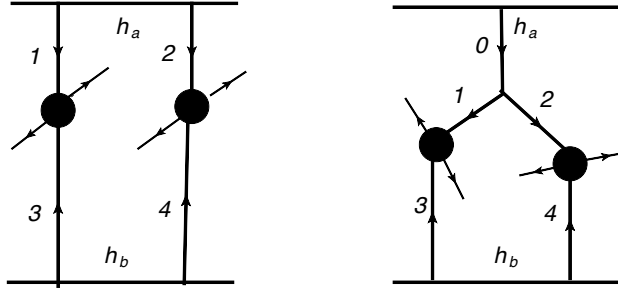


FIG. 3: Sketch of the two considered DPS mechanisms: $2 \otimes 2$ (left) and $1 \otimes 2$ (right) mechanism.

on Δ , one has to treat the two contributions separately by casting the ${}_2\text{GPD}$ as a sum of two terms depicted in Fig. 3:

$$D_h(x_1, x_2, Q_1^2, Q_2^2; \vec{\Delta}) = {}_{[2]}D_h(x_1, x_2, Q_1^2, Q_2^2; \vec{\Delta}) + {}_{[1]}D_h(x_1, x_2, Q_1^2, Q_2^2; \vec{\Delta}). \quad (13)$$

Here subscripts ${}_{[2]}D$ and ${}_{[1]}D$ mark the first and the second mechanisms, correspondingly: two partons from the wave function versus one parton that perturbatively splits into two (see Fig. 3)

Let us stress that it follows from the above formulas that in the impact parameter space these GPDs have a probabilistic interpretation. In particular they are positively definite in the impact parameter space, see discussion in [12].

B. Modeling ${}_{[2]}D$: the mean field approach.

To proceed with quantitative estimates, one needs a model for the non-perturbative two-parton distributions in a proton. A priori, we know next to nothing about them. The first natural step to take is an *approximation of independent partons*/mean field approximation. It allows one to relate ${}_2\text{GPD}$ with known objects, namely [6]

$${}_{[2]}D(x_1, x_2, Q_1^2, Q_2^2; \Delta) \simeq G(x_1, Q_1^2; \Delta^2)G(x_2, Q_2^2; \Delta^2). \quad (14)$$

Here G is the non-forward parton correlator (known as generalized parton distribution, GPD) that determines, e.g., hard vector meson production at HERA and which enter in our case in the diagonal kinematics in x ($x_1 = x'_1$).

Modeling $_2$ GPD using Eq. 14 has its limitations. First of all, it does not respect the obvious restriction $D(x_1 + x_2 > 1) = 0$. So, x_i have to be taken not too large (say, $x_i \ll 0.5$). Actually, the neglect of correlations is likely to be a good approximation only at much smaller $x \leq 0.1$. In any case, currently one can extract GPDs only from the theoretical analysis of the hard exclusive amplitude like $\gamma_L^* + N \rightarrow VM + N$ are only available for $x < 0.05$.

There is an additional caveat - in the vector meson production two gluons in t-channel carry different light cone fractions while in the case of the scattering amplitude x 's in the $|in\rangle$ and $\langle out|$ state are equal. Also, in the vector meson production modulus squared of the amplitude enters while in our case we deal with the imaginary part of the zero angle amplitude. As a result a simple connection between the gluon GPD and the observed cross section exists only if virtualities are large enough and x is small enough, $x \leq 0.1$.

On the other hand, x_i should not be *too small* to stay away from the region of the Regge-Gribov phenomena where there are serious reasons for parton correlations to be present at the non-perturbative level (see discussion in [11] and in section 6).

Thus, we expect that x -range where the mean field NP model 14 is applicable for $_2$ GPD is $10^{-1} \geq x_i \geq 10^{-3}$.

The GPDs can be parameterized as

$$G(x_1, Q_1^2; \Delta^2) \simeq D(x_1, Q_1^2) \times F_{2g}(x_1, \Delta^2, Q^2), \quad (15)$$

with D being the usual one-parton distribution functions and F being the so-called two-gluon form factor of the hadron. The latter is a non-perturbative object; it falls fast with the ‘‘momentum transfer’’ Δ^2 . In our following numerical studies we will use the model of the two gluon form factor extracted from the data on exclusive J/ψ photoproduction. This analysis is summarized in the Appendix.

Using parametrization of Eq. (7) one finds [6, 51]

$$\frac{1}{\sigma_{eff}} = \int \frac{d^2\Delta}{(2\pi)^2} F_g^4(\Delta) (8\pi B_g)^{-1} \approx 32mb, \quad (16)$$

for $x \sim 0.01$ for the exponential parametrization fit and and practically the same number, $\frac{m_g^2}{28\pi}$, for dipole fit with B_g related to m_g^2 according to Eq.56. Numerically Eq.16 leads to approximately a factor of two smaller production cross section than the one observed at the Tevatron at $x \geq 0.01$. Since the two gluon form factor decreases faster with t with decrease of x , the mean field model leads to increase of σ_{eff} with energy for the central rarities and fixed p_t . Note that the two exponential parametrization of transverse parton density used in a number of versions of Pythia which described

experimental values of σ_{eff} strongly contradicts the data on the J/ψ photoproduction, see e.g. Fig. 3 in [53].

Using Eq.12 and exponential parametrization of GPD one can also find the effective cross section for n hard collisions in mean field approach:

$$\frac{1}{\sigma_{\text{eff}}^{(n)}} = \frac{1}{(2\pi)^{N-1}} \prod_{i=1}^{i=N} \frac{1}{B_i + B'_i} \frac{1}{\sum_{i=1}^{i=N} 1/(B_i + B'_i)}. \quad (17)$$

Here $B_i \equiv B(x_i)$, $B'_i \equiv B(x'_i)$ for N dijet process with x_i are Bjorken fractions for hadron a, and x'_i are Bjorken fractions for colliding hadron b. For N=2 we get the familiar result [21]:

$$\frac{1}{\sigma_{\text{eff}}} = \frac{1}{2\pi} \frac{1}{B_1 + B'_1 + B_2 + B'_2}. \quad (18)$$

The particular case of this formula for N=3 was recently considered in [54].

IV. PQCD CORRELATIONS.

A. $1 \otimes 2$ DPS process

Actually, the NP and PT contributions *do not* enter the physical DPS cross section in the arithmetic sum Eq.13, driving one even farther from the familiar factorization picture based on universal (process independent) parton distributions. As explained in [9], a double hard interaction of two pairs of partons that *both* originate from PT splitting of a single parton from each of the colliding hadrons, does not produce back-to-back dijets. In fact, such an eventuality corresponds to a one-loop correction to the usual $2 \rightarrow 4$ jet production process and should not be looked upon as a multi-parton interaction. The term $[_1]D_{h_1} \times [_1]D_{h_2}$ has to be excluded from the product $D_{h_1} \times D_{h_2}$, the conclusion we share with Gaunt and Stirling [8].

So, we are left with two sources of genuine two-parton interactions: four-parton collisions described by the product of (PT-evolved) $_2$ GPDs of NP origin ($2 \otimes 2$),

$$[_2]D_{h_1}(x_1, x_2, Q_1^2, Q_2^2; \vec{\Delta}) [_2]D_{h_2}(x_3, x_4, Q_1^2, Q_2^2; -\vec{\Delta}), \quad (19)$$

and three-parton collisions due to an interplay between the NP two-parton correlation in one hadron and the two partons emerging from a PT parton splitting in another hadron ($1 \otimes 2$), described by the combination

$$\begin{aligned} & [_2]D_{h_1}(x_1, x_2, Q_1^2, Q_2^2; \vec{\Delta}) [_1]D_{h_2}(x_3, x_4, Q_1^2, Q_2^2; -\vec{\Delta}) \\ & + [_1]D_{h_1}(x_1, x_2, Q_1^2, Q_2^2; \vec{\Delta}) [_2]D_{h_2}(x_3, x_4, Q_1^2, Q_2^2; -\vec{\Delta}). \end{aligned} \quad (20)$$

Given that ${}_{[2]}D$ falls fast at large Δ , a mild logarithmic Δ -dependence of ${}_{[1]}D$ can be neglected in the product in Eq. 20.

B. Composition of the $1 \otimes 2$ DPS cross section

In order to derive the DPS cross section, one has to start with examination of the double differential transverse momentum distribution and then integrate it over jet imbalances δ_{ik} . Why this step is necessary? The parton distribution $D(x, Q^2)$ — the core object of the QCD-modified parton model — arises upon logarithmic integration over the transverse momentum up to the hard scale, $k_{\perp}^2 < Q^2$. Analogously, the double parton distribution $D(x_1, x_2, Q_1^2, Q_2^2; \vec{\Delta})$ embeds *independent integrations* over parton transverse momenta $k_{1\perp}^2, k_{2\perp}^2$ up to Q_1^2 and Q_2^2 , respectively. However, the $1 \otimes 2$ DPS cross section contains a specific contribution (“short split”, see below) in which the transverse momenta of the partons 1 and 2 are strongly correlated (nearly opposite). This pattern does not fit into the structure of the pQCD evolution equation for ${}_2\text{GPD}$ where $k_{1\perp}$ and $k_{2\perp}$ change independently. Given this subtlety, a legitimate question arises whether the expression for the integrated $1 \otimes 2$ cross section Eq.20 based on the notion of the two-parton distribution ${}_{[1]}D$ takes the short split into account. The differential distribution over jet imbalances was derived in [9] in the leading collinear approximation of pQCD. It resembles the “DDT formula” for the Drell-Yan spectrum [55] and contains two derivatives of the product of ${}_2\text{GPDs}$ Eq.22 that depend on the corresponding δ_{ik} as hardness scales, and the proper Sudakov form factors depending on (the ratio of) the Q_i^2 and δ_{ik}^2 .

In particular, in the region of *strongly ordered* imbalances,

$$\frac{\pi^2 d\sigma^{\text{DPS}}}{d^2\delta_{13} d^2\delta_{24}} \propto \frac{\alpha_s^2}{\delta_{13}^2 \delta_{24}^2}; \quad \delta_{13}^2 \gg \delta_{24}^2, \quad \delta_{13}^2 \ll \delta_{24}^2, \quad (21)$$

the differential $1 \otimes 2$ cross section reads

$$\begin{aligned} \frac{\pi^2 d\sigma_{1 \otimes 2}}{d^2\delta_{13} d^2\delta_{24}} &= \frac{d\sigma_{\text{part}}}{d\hat{t}_1 d\hat{t}_2} \frac{d}{d\delta_{13}^2} \frac{d}{d\delta_{24}^2} \left\{ \int \frac{d^2\vec{\Delta}}{(2\pi)^2} \right. \\ &\times {}_{[1]}D_{h_1}(x_1, x_2, \delta_{13}^2, \delta_{24}^2; \vec{\Delta}) {}_{[2]}D_{h_2}(x_3, x_4, \delta_{13}^2, \delta_{24}^2; \vec{\Delta}) \\ &\times S_1(Q_1^2, \delta_{13}^2) S_3(Q_1^2, \delta_{13}^2) \cdot S_2(Q_2^2, \delta_{24}^2) S_4(Q_2^2, \delta_{24}^2) \left. \right\} \\ &+ \{h_1 \leftrightarrow h_2\}. \end{aligned} \quad (22)$$

The differential distribution for the $2 \otimes 2$ DPS mechanism has a similar structure, see Eq. (25) of [9].

In addition to Eqs. 21,22 there is another source of double collinear enhancement in the differential $1 \otimes 2$ cross section. It is due to the kinematical region where the two imbalances nearly compensate each other,

$$\delta'^2 = (\vec{\delta}_{13} + \vec{\delta}_{24})^2 \ll \delta^2 = \delta_{13}^2 \simeq \delta_{24}^2, \quad (23)$$

and the dominant integration region is complementary to that of Eq.21:

$$\frac{\pi^2 d\sigma_{\text{short}}^{\text{DPS}}}{d^2\delta_{13} d^2\delta_{24}} \propto \frac{\alpha_s^2}{\delta'^2 \delta^2}; \quad \delta'^2 \ll \delta^2. \quad (24)$$

This enhancement characterizes the set of $1 \otimes 2$ graphs in which accompanying radiation has transverse momenta not exceeding $\vec{\delta}'$.

In this situation, the parton that compensates the overall imbalance, $\vec{k}_\perp = -\vec{\delta}'$ is radiated off the incoming, quasi-real, parton legs. At the same time, the virtual partons after the core splitting “0” \rightarrow “1” + “2” enter their respective hard collisions without radiating any offsprings on the way.

The $1 \rightarrow 2$ splitting occurs close to the hard vertices, therefore the name ”short split” (aka ”endpoint contribution”, [9]).

A complete expression for the differential distribution in the jet imbalances due to a short split was derived in the leading collinear approximation (Eq. (27) of [9]):

$$\begin{aligned} \frac{\pi^2 d\sigma_{\text{short}}^{\text{DPS}}}{d^2\delta_{13} d^2\delta_{24}} &= \frac{d\sigma_{\text{part}}}{d\hat{t}_1 d\hat{t}_2} \cdot \frac{\alpha_s(\delta^2)}{2\pi \delta^2} \sum_c P_c^{(1,2)}\left(\frac{x_1}{x_1 + x_2}\right) \\ &\times S_1(Q_1^2, \delta^2) S_2(Q_2^2, \delta^2) \\ &\times \frac{d}{d\delta'^2} \left\{ S_c(\delta^2, \delta'^2) \frac{D_{h_1}^c(x_1 + x_2, \delta'^2)}{x_1 + x_2} S_3(Q_1^2, \delta'^2) S_4(Q_2^2, \delta'^2) \right. \\ &\left. \times \int \frac{d^2\vec{\Delta}}{(2\pi)^2} [2]D_{h_2}(x_3, x_4, \delta'^2, \delta'^2; \vec{\Delta}) \right\} + \{h_1 \leftrightarrow h_2\}. \end{aligned} \quad (25)$$

The short split becomes less important when the scales of the two hard collisions are different. Indeed, the logarithmic integration over δ^2 is kinematically restricted from above, $\delta^2 < \delta_{\text{max}}^2 \simeq \min\{Q_1^2, Q_2^2\}$. As a result, in the kinematics where transverse momenta of jets in one pair are much larger than in the second pair, e.g., $Q_1^2 \gg Q_2^2$, the contribution of the short split is suppressed as

$$\sigma_{\text{short}}^{(3 \rightarrow 4)} / \sigma^{(3 \rightarrow 4)} \propto S_1(q_1^2, q_2^2) S_3(q_1^2, q_2^2) \ll 1 \quad (Q_1^2 \gg Q_2^2).$$

Here S_1 and S_3 are the double logarithmic Sudakov form factors of the partons “1” and “3” that enter the hard interaction with the larger hardness scales. The short split induces a strong correlation between jet imbalances which is worth trying to look for experimentally.

The relative weight of the short split depends on the process under consideration. For most DPS processes in the kinematical region we have studied, it typically provides 10–15% of the pQCD correlation contribution. However, it becomes more important when the nature of the process favors parton splitting. In particular, this is the case for the double Drell-Yan pair production where the short split contribution reaches 30–35%. On the contrary, the short split turns out to be practically negligible for the same-sign double W -meson production [12].

Thus, for the integrated DPS cross section we obtain two contributions to the effective interaction area:

$$\begin{aligned} \frac{\prod_{i=1}^4 D(x_i)}{\sigma_4} &= \int \frac{d^2 \vec{\Delta}}{(2\pi)^2} [2]D_{h_1}(x_1, x_2, Q_1^2, Q_2^2; \vec{\Delta}) [2]D_{h_2}(x_3, x_4, Q_1^2, Q_2^2; -\vec{\Delta}), \\ \frac{\prod_{i=1}^4 D(x_i)}{\sigma_3} &= \int \frac{d^2 \vec{\Delta}}{(2\pi)^2} \left[[2]D_{h_1}(x_1, x_2, Q_1^2, Q_2^2; \vec{\Delta}) [1]D_{h_2}(x_3, x_4, Q_1^2, Q_2^2) \right. \\ &\quad \left. + [1]D_{h_1}(x_1, x_2, Q_1^2, Q_2^2) [2]D_{h_2}(x_3, x_4, Q_1^2, Q_2^2; \vec{\Delta}) \right]. \end{aligned} \quad (26)$$

Let us stress here that our analysis demonstrates that a compact and intuitively clear expression containing the product of the ${}_2$ GPDs $[2]D$ and $[1]D$ in Eq.26 is valid only for the *integrated* $1 \otimes 2$ cross section.

C. Modeling ${}_1D$ terms.

Turning to the $1 \otimes 2$ term, we neglect a mild logarithmic Δ -dependence of $[1]D$ in 26 and use the model of section 3B for $[2]D$ to obtain

$$\sigma_3^{-1} \simeq \frac{7}{3} \cdot \left[\frac{[1]D(x_1, x_2)}{D(x_1)D(x_2)} + \frac{[1]D(x_3, x_4)}{D(x_3)D(x_4)} \right] \times \sigma_4^{-1}, \quad (27)$$

where we substituted the value of the integral

$$\int \frac{d^2 \vec{\Delta}}{(2\pi)^2} F_{2g}^2(\Delta^2) = \frac{m_g^2}{12\pi}.$$

Very similar results are obtained for exponential parametrisation.

We will parametrize the result in terms of the ratio

$$R \equiv \frac{\sigma_{1 \otimes 2}}{\sigma_{2 \otimes 2}} = \frac{\sigma_4}{\sigma_3}. \quad (28)$$

For the effective interaction area,

$$\sigma_{\text{eff}}^{-1} = \sigma_4^{-1} + \sigma_3^{-1}, \quad (29)$$

we parametrize

$$\sigma_{eff} = \frac{\sigma_{eff}^{\text{mean field}}}{1 + R}, \quad (30)$$

where $\sigma_{eff}^{\text{meanfield}}$ is the mean field value of σ_{eff} , obtained either using dipole or exponential fit. The difference between the values for σ_{eff} obtained using these two fits is within current experimental errors of the J/ψ data. In numerical simulations for DPS below we use dipole fit, that works slightly better for values of Bjorken x corresponding to hard DPS, while for the underlying event (UE) we used the exponential fit, that works slightly better for small x relevant for the UE. The difference however is of the order of several percent and can be neglected.

Within the framework of the NP two-parton ${}_2\text{GPD}$ model, Eq.14, there is only one free parameter Q_0^2 . The DPS theory can be applied to various processes and holds in a range of energies and different kinematical regions. Therefore, having fixed the Q_0^2 value, say, from the Tevatron data, one can consider all other applications (in particular, to the LHC processes) as parameter-free theoretical predictions.

D. Analytical estimate of pQCD correlations.

The PT parton correlations cannot be neglected. Indeed, let us chose a scale Q_0 that separates NP and PT physics to be sufficiently low, so that parton cascades due to the evolution between Q_0 and Q_i^2 are well developed. To get a feeling of the relative importance of the PT correlation, as well as to understand its dependence on x and the ratio of scales, Q^2 vs Q_0^2 , the following lowest order PT estimate can be used.

Imagine that at the scale Q_0 the nucleon consisted of n_q quarks and n_g gluons ("valence partons") with relatively large longitudinal momenta, so that triggered partons with $x_1, x_2 \ll 1$ resulted necessarily from PT evolution. In the first logarithmic order, $\alpha_s \log(Q^2/Q_0^2) \equiv \xi$, the inclusive spectrum can be represented as

$$D \propto (n_q C_F + n_g N_c) \xi,$$

where we suppressed x -dependence as irrelevant. If both gluons originate from the same "valence" parton, then

$${}_{[1]}D \propto \frac{1}{2} N_c \xi \cdot D + (n_q C_F^2 + n_g N_c^2) \xi^2, \quad (31)$$

while independent sources give:

$${}_{[2]}D \propto (n_q(n_q-1)C_F^2 + 2n_qn_gC_FN_c + n_g(n_g-1)N_c^2)\xi^2 = D^2 - (n_qC_F^2 + n_gN_c^2)\xi^2. \quad (32)$$

Hence

$$cD(x_1, x_2; 0)D(x_1)D(x_2) - 1 \simeq \frac{N_c}{2(n_qC_F + n_gN_c)}. \quad (33)$$

The correlation is driven by the gluon cascade — the first term in Eq.31 — and is not small (being of the order of unity). It gets diluted when the number of independent “valence sources” at the scale Q_{02} increases. This happens, obviously, when x_i are taken smaller. On the other hand, for large $x_i \sim 0.1$ and increasing, the effective number of more energetic partons in the nucleon is about two and decreasing, so that the relative importance of the $1 \otimes 2$ processes grows.

We conclude that the relative size of PT correlations is of the order one, provided $\xi = \mathcal{O}(1)$.

V. NUMERICAL RESULTS FOR DPS

A. Calculation framework

We consider in this chapter hard DPS with $p_t > 10 \div 15$ GeV, where the $1 \otimes 2$ mechanism gives the dominant correction to the mean field results.(The pattern for small p_t relevant for UE is discussed in the next section). In numerical calculations we used the GRV92 parametrization of gluon and quark parton distributions in the proton [56]. We have checked that using more advanced GRV98 and CTEQ6L parametrizations does not change the numerical results. The explicit GRV92 parametrization is speed efficient and allows one to start the PT evolution at rather small virtuality scales. The combination $(Q_0^2 + \Delta^2)$ was used as the lower cutoff for the logarithmic transverse momentum integrals in the parton evolution, which induced a mild (logarithmic) Δ -dependence on top of the relevant power of the two-gluon form factor $F_{2g}(\Delta^2)$.

To quantify the role of the $1 \otimes 2$ DPS subprocesses, we calculated the ratio R defined in Eq. 28 in the kinematical region $10^{-3} \leq x_i \leq 10^{-1}$ for Tevatron ($\sqrt{s} = 1.8 \div 1.96$ TeV) and LHC energies ($\sqrt{s} = 7$ TeV). We chose to consider three types of ensembles of colliding partons:

1. $u(\bar{u})$ quark and three gluons which is relevant for “photon plus 3 jets” CDF and D0 experiments,
2. four gluons (two pairs of hadron jets),

3. $u\bar{d}$ plus two gluons, illustrating W^+jj production.
4. $u\bar{d}$ plus $d\bar{u}$, corresponding to the W^+W^- channel.

B. Perturbative $1 \otimes 2$ correlation at the Tevatron.

1. CDF experiment

In Fig. 4 we show the profile of the $1 \otimes 2$ to $2 \otimes 2$ ratio R for the $\gamma + 3$ jets process in the kinematical domain of the CDF experiment [29]. The calculation was performed for the dominant ‘‘Compton scattering’’ channel of the photon production: $g(x_2) + u(\bar{u})(x_4) \rightarrow \gamma + u(\bar{u})$. The longitudinal momentum fractions of two gluons producing second pair of jets are x_1 and x_3 . The typical transverse momenta were taken to be $p_{\perp 1,3} \simeq 5$ GeV for the jet pair, and $p_{\perp 2,4} \simeq 20$ GeV for the photon–jet system. In Fig. 4 R is displayed as a function of rapidities of the photon–jet, $\eta_2 = \frac{1}{2} \ln(x_2/x_4)$, and the 2-jet system, $\eta_1 = \frac{1}{2} \ln(x_1/x_3)$.

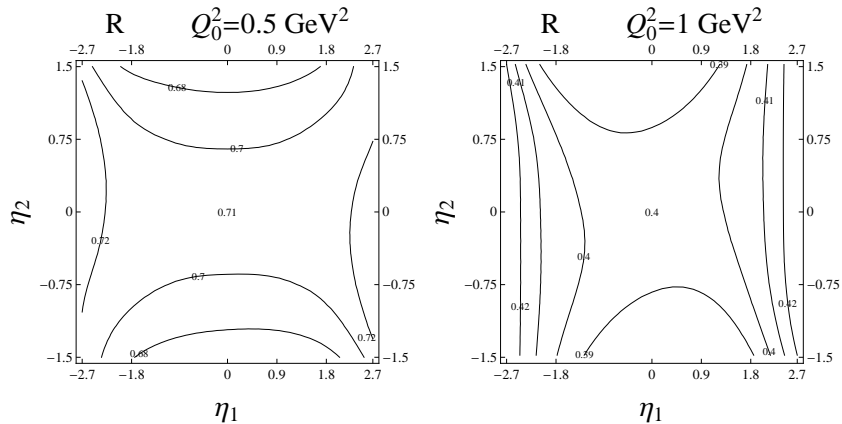


FIG. 4: The $1 \otimes 2/2 \otimes 2$ ratio, Eq.28 in the CDF kinematics for the process $p\bar{p} \rightarrow \gamma + 3 \text{ jets} + X$.

We observe that the enhancement factor lies in the ballpark of $1 + R \sim 1.5 \div 1.8$. Processed through Eq. 30, it translates into $\sigma_{\text{eff}} \simeq 18 \div 21$ mb. This expectation has to be compared with the CDF finding $\sigma_{\text{eff}} = 14.5 \pm 1.7^{+1.7}_{-2.3}$ mb. A recent reanalysis of the CDF data points at an even small value: $\sigma_{\text{eff}} = 12.0 \pm 1.4^{+1.3}_{-1.5}$ mb, [45]. Both these values are significantly smaller than our estimate and the result of D0 experiment discussed in the next subsection.

The results of numerical calculation for a fixed hardness Q^2 are shown in Fig. 4 for the CDF kinematics. We find that the R factor and hence σ_{eff} exhibits a very mild x -dependence.

2. D0 experiment

The ratio R is practically constant in the kinematical domain of the D0 experiment which studied photon+3 jets production [30, 31] and is very similar to that of the CDF experiment shown above in Fig. 4. So, for the D0 kinematics we instead display in Fig. 5 the enhancement factor $1+R$ as a function of p_{\perp} of the secondary jet pair for photon transverse momenta 10, 20, 30, 50, 70, and 90 GeV (from bottom to top).

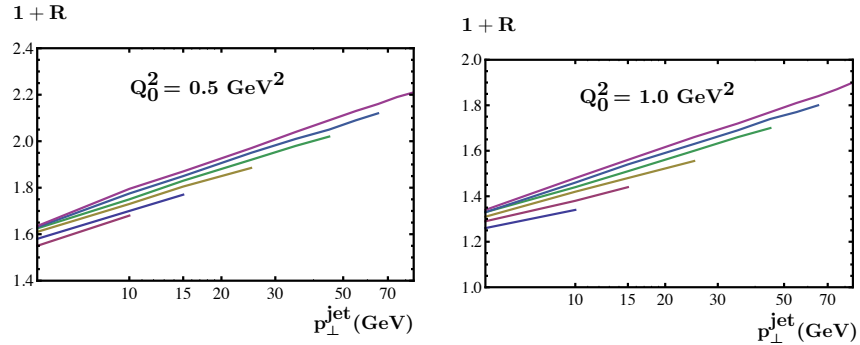


FIG. 5: left: Central rapidity photon+3 jets production in $u(\bar{u})$ -gluon collisions in the D0 kinematics for $Q_0^2 = 0.5\text{GeV}^2$. Right: for $Q_0^2 = 1\text{GeV}^2$.

The corresponding prediction for σ_{eff} is shown in Fig. 6 in comparison with the D0 findings.

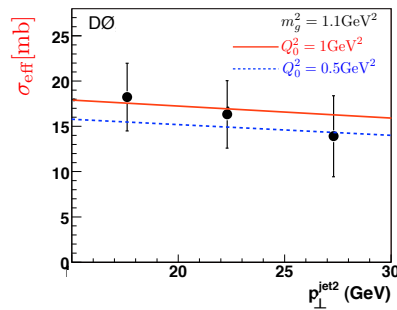


FIG. 6: σ_{eff} as a function of the hardness of the second jet in the kinematics of the D0 experiment [30, 31] for $p_{\perp\gamma} = 70\text{ GeV}$.

Both the absolute value and the hint of decrease of σ_{eff} with increase of p_{\perp} look satisfactory.

C. LHC energies

In Fig. 7 we show the $1 \otimes 2$ to $2 \otimes 2$ ratio for production of two pairs of back-to-back jets with transverse momenta 50 GeV produced in collision of gluons at the LHC energy of $\sqrt{s} = 7\text{ TeV}$ (the pattern for higher LHC energies is very similar).

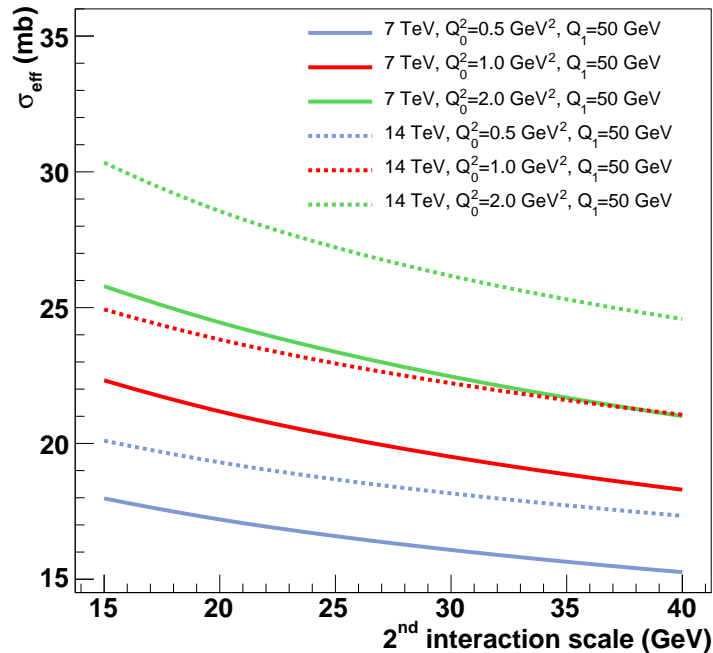


FIG. 8: σ_{eff} for two dijets in DPS at the LHC.

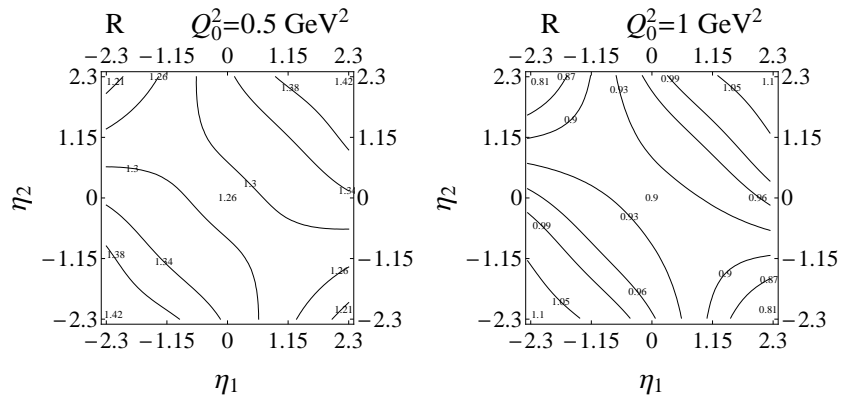


FIG. 7: Rapidity dependence of the R factor for two pairs of $p_{\perp} = 50$ GeV jets produced in gluon-gluon collisions

Dependence on the hardness parameters of the DPS process of double gluon-gluon collisions is illustrated in Fig. 8. For the sake of illustration, we have chosen the value of the p_{\perp} cutoff parameter, varied $Q_0^2 = 0.5, 1, 2$ GeV², and calculated the σ_{eff} as a function of transverse momenta of the second dijet. [21]

For considered \sqrt{s}, p_{\perp} range, R increases by about 15–25% with increase of the hardness of one of the jet pairs. This corresponds to approximately 10% drop of σ_{eff} .

Finally, in Fig. 9 we show the rapidity profile of the R ratio for the process of production of the vector boson, $u\bar{d} \rightarrow W^+$, accompanied by an additional pair of (nearly back-to-back) jets with transverse momenta $p_{\perp} \simeq 30$ GeV produced in a gluon-gluon collision.

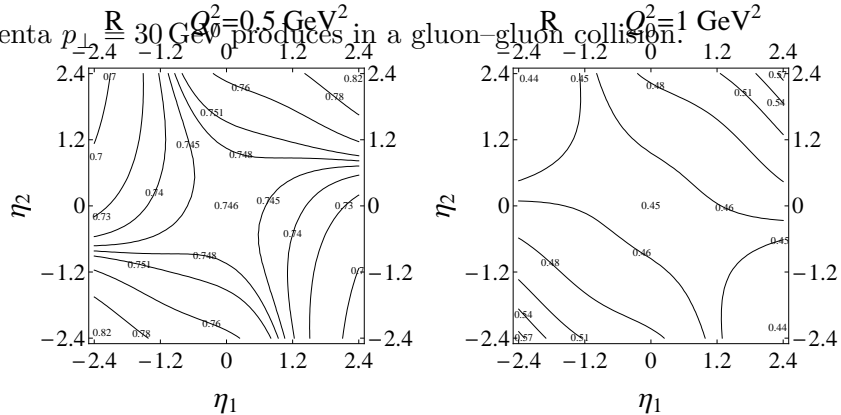


FIG. 9: Ratio R for production of W plus a pair of $p_{\perp} \simeq 30$ GeV gluon jets

It is interesting to notice that the effect of perturbatively induced parton-parton correlations is maximal for equal rapidities of the W and the jet pair, and slowly diminishes when they separate. This feature is more pronounced when the cutoff parameter Q_0^2 is taken larger. In this case the PT correlation becomes smaller and, at the same time, exhibits a stronger rapidity dependence.

The recent ATLAS study [34] reported for this process the value $\sigma_{\text{eff}} = 15 \pm 3^{+5}_{-3}$ mb which is consistent with the expected enhancement due to contribution of the $1 \otimes 2$ DPS channel, see Eq. 28. The characteristic feature of our approach is that σ_{eff} depends both on the longitudinal fractions and transverse scale. For example, consider Wjj processes: Fig. 10 presents the dependence of σ_{eff} on the transverse momenta of jets of the second pair, $p_{\perp} \equiv p_{\perp 2}$.

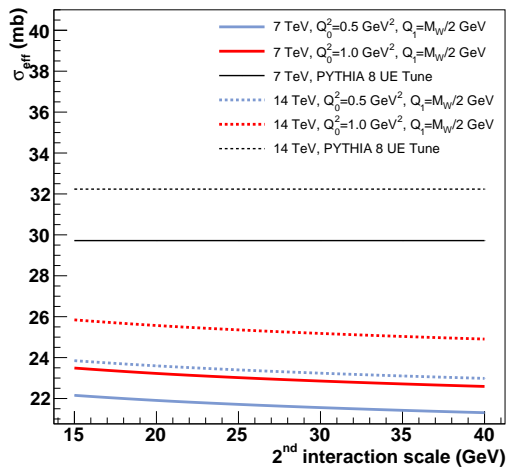


FIG. 10: σ_{eff} for Wjj processes as function of a transverse scale of a dijet.

We observe that within the considered kinematic range, R increases by about 15–25% with increase of the hardness of one of the jet pairs. This corresponds to approximately 10% decrease of σ_{eff} . It is interesting to notice that the effect of perturbatively induced parton–parton correlations is maximal for equal rapidities of the W and the jet pair, and diminishes with increase of the rapidity interval between W and $2j$. This feature is more pronounced when the cutoff parameter Q_0^2 is taken larger, so that the pQCD correlation becomes smaller and, at the same time, exhibits a stronger rapidity dependence.

Theoretical derivation of the effective interaction area σ_{eff} (“effective cross section”) in [6, 9, 11, 12] relied on certain assumptions and approximations. Our approach to perturbative QCD effects in DPS developed in [9] was essentially probabilistic. In particular, we did not discuss the issue of possible interference between $1 \otimes 2$ and $2 \otimes 2$ two-parton amplitudes. One can argue that such eventuality should be strongly suppressed. Indeed, spatial properties of accompanying radiation produced by so different configurations make them unlikely to interfere, since in the $2 \otimes 2$ mechanism a typical transverse distance between two partons from the hadron w.f. is of order of the hadron size, while in the $1 \otimes 2$ case it is much smaller and is determined by a hard scale. Moreover, we disregarded potential contributions from non-diagonal interference diagrams that are due to crosstalk between partons in the amplitude and the conjugated amplitude. Such contributions appear to be negligible in the kinematic region under consideration [18].

Finally, our prediction for the DPS cross sections was based on a model assumption of the absence of NP two-parton correlations in the proton. This assumption is the simplest guess. One routinely makes it due to the lack of any firsthand information about such correlations. In [11] we have pointed out a source of genuine non-perturbative two-parton correlations that should come into play for very small x values, $x \ll 10^{-3}$, and estimated its magnitude via inelastic diffraction in the framework of the Regge–Gribov picture of high energy hadron interactions. The theory of small x NP correlations and their role are discussed in the next chapter.

In order to be able to reliably extract the DPS physics, one has to learn how to theoretically predict contribution of two parton collision with production of two hard systems (four jets in particular). This is the dominant channel, and it is only in the back-to-back kinematics that the $2 \otimes 2$ and $1 \otimes 2$ DPS processes become competitive with it. Among first subleading pQCD corrections to the $1 \otimes 1$ amplitude, there is a loop graph that looks like a two-by-two parton collision. However this resemblance is deceptive. Unlike the $2 \otimes 2$ and $1 \otimes 2$ contributions, this specific correction does not depend on the spatial distribution of partons in the proton (information encoded in σ_{eff}), it is not power enhanced in the region of small transverse momenta of hard systems, and therefore

does not belong to the DPS mechanism [6, 8, 9]. Treating the the amplitude corresponding to splitting of two incoming partons at the one –lop level, corresponds to the two-loop accuracy for the cross section. Until this accuracy is achieved, the values of σ_{eff} extracted by experiments should be considered as tentative.

Our first conclusion is that in the kinematical region explored by the Tevatron and the LHC experiments, the x -dependence of σ_{eff} turns out to be rather mild. This by no means implies, however, that σ_{eff} can be looked upon as any sort of a universal number. On the contrary, we see that the presence of the perturbative correlation due to the $1 \otimes 2$ DPS mechanism results in the dependence of σ_{eff} not only on the parton momentum fractions x_i and on the hardness parameters, but also on the type of the DPS process.

For example, in the case of golden DPS channel of production of two same sign W bosons [5] the discussed mechanism leads to expectation of significantly larger σ_{eff} than for, say, W plus two jets process. Indeed, the comparison of the values of R for central production of two gluon jet pairs, Wjj and W^+W^+ (with jet transverse momenta $p_{\perp} \simeq M_W/2$), gives ($\sqrt{s} = 7 \text{ TeV}$, $\eta_1 = \eta_2 = 0$)

$$\begin{aligned} qR(jj + jj) &= 1.18 \quad (0.81) \\ R(W + jj) &= 0.75 \quad (0.45) \\ R(W^+W^+) &= 0.49 \quad (0.26) \end{aligned} \tag{34}$$

for $Q_0^2 = 0.5 \text{ (1.0) GeV}^2$. As a result of the different magnitude of the perturbative correlation contribution for different processes, the effective interaction areas σ_{eff} comes out to be significantly different for the three processes:

$$\begin{aligned} jj + jj : \quad \sigma_{\text{eff}} &= 14.5 \div 20 \text{ mb}, \\ W + jj : \quad \sigma_{\text{eff}} &= 20 \div 23.5 \text{ mb}, \\ W^+W^+ : \quad \sigma_{\text{eff}} &= 21.5 \div 25.4 \text{ mb}. \end{aligned} \tag{35}$$

In all cases the effective cross section is smaller for lower Q_0^2 due to a more developed perturbative parton cascades.

In difference from the W^+W^+ channel, the *double Drell-Yan process* favors the $1 \otimes 2$ mechanism, $g \rightarrow u\bar{u}$. As a result, the effective interaction area in this case turns out to be significantly smaller. For example, for the central production of two Z bosons at $\sqrt{s} = 7 \text{ TeV}$ we find

$$R(ZZ) = 1.03 \quad (0.73), \text{ corresponding to } \sigma_{\text{eff}}(ZZ) = 15.9 \div 18.5 \text{ mb}. \tag{36}$$

The results for σ_{eff} for higher LHC energies are quite close (within the accuracy of measurements), cf. Figs. 8, 10, and have similar pattern.

We mentioned above that an important feature of the $1 \otimes 2$ mechanism is its dependence on the hardness of the process. With increase of Q_i^2 , the $1 \otimes 2$ to $2 \otimes 2$ ratio R is predicted to increase rather rapidly, resulting in smaller values of σ_{eff} . At the same time, with decrease of the p_{\perp} of the jets this contribution decreases. We have seen above, that such a trend is consistent with the D0 data for $x \geq 10^{-2}$, Fig. 6.

VI. NON-FACTORIZED CONTRIBUTION TO ${}_2D$ AT THE INITIAL Q_0 SCALE.

A. Basic ideas

There is an additional contribution to the DPS at small x which is related to the soft dynamics. It was first discussed in [11], and in a more detail in [23]. It was demonstrated in [23] that soft dynamics leads to positive correlations between partons at small x which have to be included in the calculation of the DPS cross section. These soft correlations can be calculated using the connection between correlation effects in MPI and inelastic diffraction. The emerging non-factorized contribution to ${}_2\text{GPD}$ is calculated at the initial scale Q_0^2 that separates soft and hard physics and which we consider as the starting scale for the DGLAP evolution. One expects that for this scale the single parton distributions at small x are given by the soft Pomeron and soft Reggeon exchange.

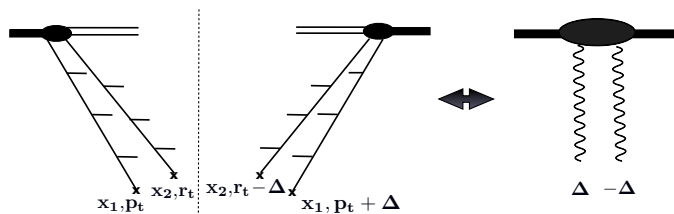


FIG. 11: ${}_2\text{GPD}$ as a two Pomeron exchange

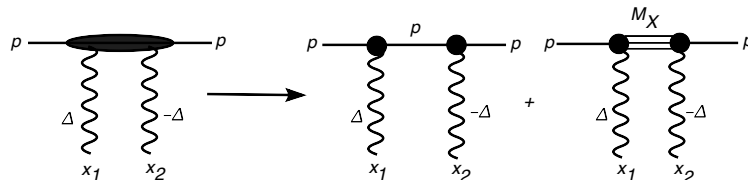


FIG. 12: $2IP$ contribution to ${}_2D$ and corresponding Reggeon diagrams

The diagrams of Fig. 11,12 lead to a simple expression for the non-factorizable/correlated con-

tribution. (see [23] for details). For the correlated contribution we have,

$$\begin{aligned} {}_2D(x_1, x_2, Q_0^2)_{nf} &= c_{3P} \int_{x_m/a}^1 \frac{dx}{x^2} D(x_1/x, Q_0^2) D(x_2/x, Q_0^2) \left(\frac{1}{x}\right)^{\alpha_P}. \\ &+ c_{PPR} \int_{x_m/a}^1 \frac{dx}{x^2} D(x_1/x, Q_0^2) D(x_2/x, Q_0^2) \left(\frac{1}{x}\right)^{\alpha_R}. \end{aligned} \quad (37)$$

Here $x_m = \max(x_1, x_2)$. We also introduced an additional factor of $a = 0.1$ in the limit of integration over x (or, equivalently, the limit of integration over diffraction masses M^2) to take into account that the Pomeron exchanges occupy at least two units in rapidity, i.e. $M^2 < 0.1 \cdot \min(s_1, s_2)$ ($s_{1,2} = m_0^2/x_{1,2}$), or $x > \max(x_1, x_2)/0.1$, where $m_0^2 = m_N^2 = 1 \text{ GeV}^2$ is the low limit of integration over diffraction masses. Here c_{3P} and c_{PPR} are normalized three Pomeron and Pomeron-Pomeron-Reggeon vertices. We determine c_{3P} and c_{PPR} from the HERA data [57] for the ratio of inelastic and elastic diffraction at $t = 0$: $\omega \equiv \frac{d\sigma_{in. dif.}}{d\sigma_{el}} \Big|_{t=0} = 0.25 \pm 0.05$, and from analysis of diffraction for large x carried in [58], which shows that $c_{PPR} \sim 1.5c_{3P}$. We are considering here relatively low energies (relative large x) and a rather modest energy interval. Hence we neglect energy dependence of c_{3P} . Numerically, we obtain $c_{3P} = 0.075 \pm 0.015$, $c_{PPR} \sim 0.11 \pm 0.03$ for $Q_0^2 = 0.5 \text{ GeV}^2$ and $c_{3P} = 0.08 \pm 0.015$ and $c_{PPR} = 0.12 \pm 0.03$ for $Q_0^2 = 1. \text{ GeV}^2$, using the Pomeron intercept values given below. Note that the intercept of the Pomeron that splits into 2 (region between two blobs in fig. 3) is always 1.1 for $t = 0$, i.e. this Pomeron is by definition soft, and the intercept of the Reggeon is 0.5.

For the parton density in the ladder we use [23]: $x D(x, Q_0^2) = \frac{1-x}{x^{\lambda(Q_0^2)}}$, where the small x intercept of the parton density λ is taken from the GRV parametrization [59] for the nucleon gluon pdf at Q_0^2 at small x . Numerically $\lambda(0.5\text{GeV}^2) \sim 0.27$, $\lambda(1.0\text{GeV}^2) \sim 0.31$.

Consider now the $t = -\Delta^2$ dependence of the above expressions. The t -dependence of the factorized contribution to ${}_2D_f$ is given by

$$F(t) = F_{2g}(x_1, t) \cdot F_{2g}(x_2, t) = \exp((B_{el}(x_1) + B_{el}(x_2))t/2), \quad (38)$$

where F_{2g} is the two gluon nucleon form factor. The t -dependence of the non-factorized term Eq. 37 is given by the t -dependence of the inelastic diffraction: $\exp(B_{in}t)$. Using the exponential parameterization $\exp(B_{in}t)$ for the t -dependence of the square of the *inelastic vertex* $pM_X P$, the experimentally measured ratio of the slopes $B_{in}/B_{el} \simeq 0.28$ [60] translates into the absolute value $B_{in} = 1.4 \div 1.7 \text{ GeV}^2$.

The evolution of the initial conditions, Eq. 37, is given by

$${}_2D(x_1, x_2, Q_1^2, Q_2^2)_{nf} = \int_{x_1}^1 \frac{dz_1}{z_1} \int_{x_2}^1 \frac{dz_2}{z_2} G(x_1/z_1, Q_1^2, Q_0^2) G(x_2/z_2, Q_2^2, Q_0^2)$$

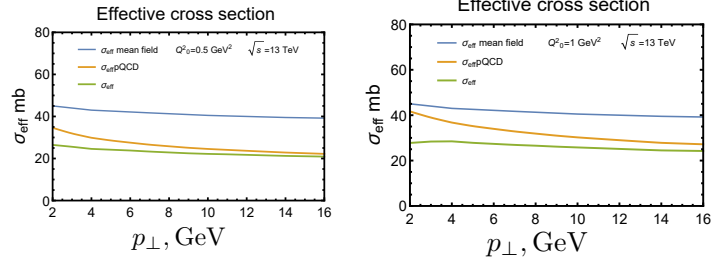


FIG. 13: σ_{eff} as a function of the transverse scale p_{\perp} for $Q_0^2 = 0.5$ (left), and $Q_0^2 = 1$ GeV^2 (right) in the central kinematics. We present the mean field, the mean field plus $1 \otimes 2$ mechanism and total σ_{eff} for $\sqrt{s} = 13$ TeV.

$$\times {}_2D(z_1, z_2, Q_0^2)_{\text{nf}}, \quad (39)$$

where $G(x_1/z_1, Q_1^2, Q_0^2)$ is the conventional DGLAP gluon-gluon kernel [55] which describes evolution from Q_0^2 to Q_1^2 . In our calculation we neglect initial sea quark densities in the Pomeron at scale Q_0^2 (obviously Pomeron does not receive contribution from the valence quarks). We refer to [28] for numerical calculation of K .

B. σ_{eff} in the central kinematics

. The enhancement coefficient is now given by the

$$R = R_{pQCD} + R_{soft}. \quad (40)$$

where R_{pQCD} corresponds to the contribution of $1 \otimes 2$ pQCD mechanism (Fig. 3 right) and was calculated in [12], while the expression for R_{soft} is given by

$$R_{soft} = \frac{4K}{1 + B_{inel}/B_{el}} + \frac{K^2 B_{el}}{B_{in}} + KR_{pQCD}B_{el}/B_{inel}, \quad (41)$$

where we calculate all factors for $x_1 = x_2 = x_3 = x_4 = \sqrt{4Q^2/s}$, with s being invariant energy of the collision. We present our numerical results in Figs. 13,14:

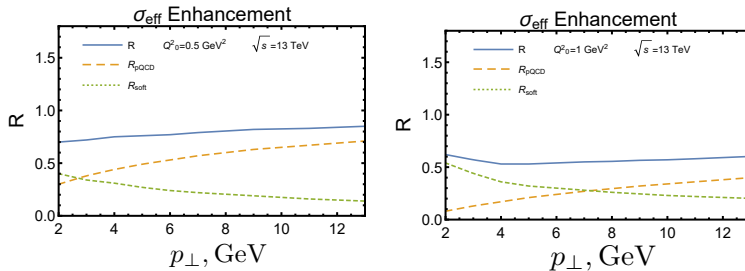


FIG. 14: R for different Q_0^2 and $\sqrt{s} = 13$ TeV.

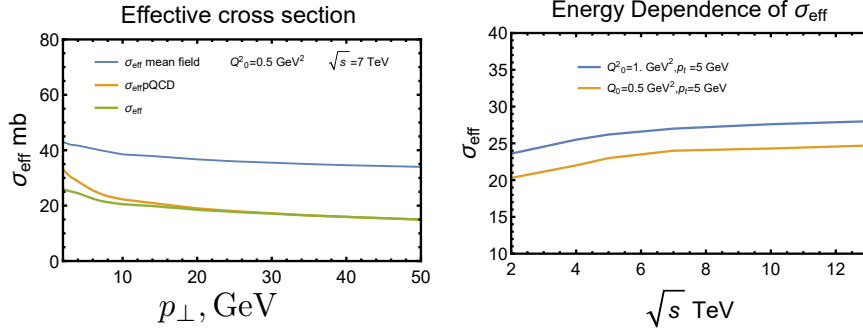


FIG. 15: left: σ_{eff} for the entire transverse momenta region ($Q_0^2 = 0.5 \text{ GeV}^2$), right: The characteristic energy dependence of σ_{eff} on c.m.s. energy \sqrt{s} .

In addition, in order to illustrate the picture of σ_{eff} behavior in both UE and DPS, in Fig. 13 we give the example of the p_{\perp} dependence of σ_{eff} for the transverse momenta region 2–50 GeV for $Q_0^2 = 0.5 \text{ GeV}^2$ (for $Q_0^2 = 1 \text{ GeV}^2$ the behavior is very similar).

We also studied the energy dependence of σ_{eff} for fixed transverse momenta p_{\perp} on s in the UE kinematic region in the energy region from Tevatron to LHC. We find that σ_{eff} slowly increases with s and practically flattens out at the top of the LHC energies, see Fig. 15 right.

In order to understand the evolution of σ_{eff} at higher incident energies for given transverse scale we would need the information on the x dependence of the two-gluon form factor for small $x \leq 10^{-4}$ and of the inelastic diffraction which are likely to come from the current analyses of the J/ψ diffractive production in the ultraperipheral collisions at the LHC.

Our current estimates of non-factorizable contribution should be considered as semiquantitative due to the large uncertainties in diffraction parameters as well as the use of the "effective" values for the reggeon/pomeron parameters (which include screening corrections very roughly). Nevertheless, our results indicate a number of basic features of soft nonperturbative parton - parton correlations which are relevant for the central LHC dynamics.

(i) For large transverse momenta, relevant for hard DPS scattering, soft effects are small and essentially negligible, contributing only 5% to the enhancement coefficient R if we start evolution at the scale $Q_0^2 = 0.5 \text{ GeV}^2$, and 10 – 15% for the starting scale of 1 GeV^2 , for $p_{\perp} \sim 15 - 20 \text{ GeV}$. Thus they do not influence detailed hard DPS studies described in the previous sections. Our results also indicate that the characteristic transverse momentum p_{t0} , for which soft correlations constitute given fixed fraction of the enhancement factor R rapidly increase with s .

(ii) The soft non-factorizable contributions may contribute significantly in the underlying event dynamics, especially at the scales $p_{\perp} = 2 \div 4 \text{ GeV}$ where they are responsible for about 50% of the

difference between mean field result and full prediction for σ_{eff} for $Q_0^2=0.5 \text{ GeV}^2$ case. If we would start evolution at $Q_0^2 = 1 \text{ GeV}^2$, soft effects would dominate up to scale $p_\perp \sim 4 \text{ GeV}$. In the UE the account of the soft contribution leads to stabilization of the results for σ_{eff} , and to its slower decrease with increase of p_\perp than in the approximation in which only perturbative correlations, i.e. the $1 \otimes 2$ mechanism is included. These values for σ_{eff} for UE, especially for scales 2–4 GeV are very close to the ones used by Pythia.

We see that the new framework gives a reasonable description of the data over the full transverse momenta range, with weaker dependence of the quality of the fit on the starting point of the evolution Q_0 than in [21].

(iii) The evolution of σ_{eff} with transverse scale is stabilized for the UE regime, as shown in Fig. 13 leading to an almost plateau like behavior with a slight decrease with increase of the transverse scale.

(iv) The inclusion of the soft correlations stabilizes the incident energy dependence of σ_{eff} . It changes only slightly between 3.5 TeV and 6.5 TeV proton collision energies for the same transverse scale for small p_\perp . In other words, the increase of the soft correlations compensates the decrease of the relative pQCD contribution with an increase of the collision energy due to decrease of effective x_i .

We refer the reader to the original papers [27, 28] for more details.

One of the processes which is sensitive to the non-factorizable contribution is production of double open charm in the forward kinematics which was recently studied in the LHCb experiment. We find that the mean field approximation for the double parton GPD, which neglects parton-parton correlations, underestimates the observed rate by a factor of two. The enhancement due to the perturbative QCD correlation $1 \otimes 2$ mechanism which explains the rate of double parton interactions at the central rapidities is found to explain 60 ÷ 80 % of the discrepancy. We find [27] that non-factorized contributions to the initial conditions for the DGLAP collinear evolution of the double parton GPD discussed above play an important role in this kinematics. Combined, the two correlation mechanisms provide a good description of the rate of double charm production reported by the LHCb[37] with the result weakly sensitive to the starting point of the QCD evolution. At the same time we cannot reproduce small values of σ_{eff} for the double J/ψ channel reported by the LHCb which may indicate a more complicated pQCD of charmonium production.

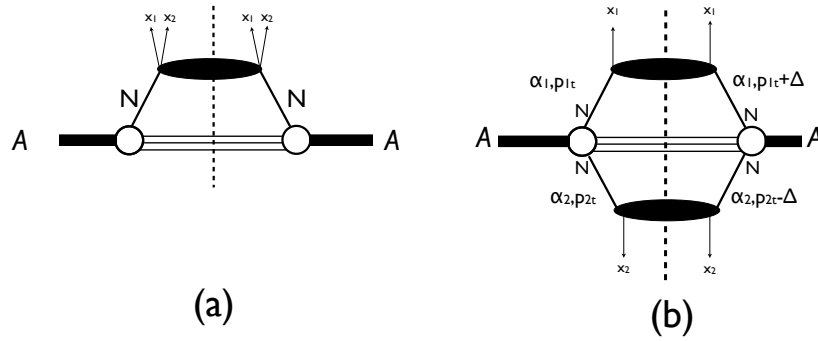


FIG. 16: Impulse approximation and two nucleon contributions to DPS in pA scattering

VII. MPI IN PROTON - NUCLEUS SCATTERING

Above we considered the case of pp scattering. The same formalism is applicable for collision of any two hadrons and in particular for the proton - nucleus scattering. Cross sections of the MPI processes for the pA case were first calculated in the parton model approximation in [24]. It was demonstrated that the double, triple,... MPI are strongly enhanced in the proton collisions with heavy nuclei due to a possibility of hard collisions occurring simultaneously on 2 (3,...) nucleons at the same impact parameter. It was also emphasized that a comparison of the MPI in pp and pA scattering would allow to study longitudinal correlations of partons in nucleons [24]. Further, it was demonstrated in [25] that corrections to the parton model expression in the mean field approximation are much smaller than in the pp case.

The technique we described in section 2 allows to perform the calculation in a very compact form [25]. We will focus on the case of DPS. In this case we have two contributions - the impulse approximation, corresponding to two partons of the nucleus involved in the collision belonging to the same nucleon (Fig. 16a), σ_1 :

$$\sigma_1 = A\sigma_{NN} \quad (42)$$

and two different nucleons, σ_2 (Fig. 16b). Since the b -dependence of the nuclear density is much slower than that for the nucleon σ_2 is not sensitive to the transverse distance between the partons of the nucleon and hence proportional to the double parton distribution. Picking up two partons at similar impact parameters in the heavy nucleus is $\propto A^{4/3}$, leading to $\sigma_2/\sigma_1 \propto A^{1/3}$

For simplicity we restrict the discussion to the case of $x_i^{(A)} \geq 0.01$ where interference effects corresponding to $x_1^{(A)}(x_2^{(A)})$ belongs to one nucleon in the $|in\rangle$ state and to another nucleon in the $\langle out|$ state. For analysis of the effect of the leading twist nuclear shadowing see [61].

Similar to the pp case, the expression for σ_2 is proportion to the integral over Δ of the product of the double GPDs of proton and nucleus. The two GPD form factor of the nucleus is

$${}_2GPD_A(\Delta) = F_A(\Delta, -\Delta) \cdot F_g^2(\Delta, x). \quad (43)$$

Here $F_A(\Delta, -\Delta)$ is the two body nuclear form factor. In the mean field approximation for the nucleus wave function:

$$F_A(\Delta, -\Delta) = A^2 F_A^2(\Delta) \approx A^2 \exp(-R_A^2 \Delta^2/3), \quad (44)$$

where $F_A(\Delta)$ is the nucleus single body form factor normalized to one at $\Delta = 0$. Since the Δ^2 dependence of $F_A^2(\Delta)$ is much stronger than that of $F_g^4(\Delta, x)$ the later can be neglected in the integral

$$\int d^2\Delta {}_2GPD(\Delta, N) \cdot {}_2GPD(\Delta, A) = \int d^2A^2 \Delta F_A^2(\Delta). \quad (45)$$

It is convenient at this point to switch to the impact parameter representation using $\int d^2\Delta A^2 F_A^2(\Delta) = \int d^2b T_A^2(b)$, where $T_A(b)$ is the nuclear thickness function normalized to A: $\int d^2b T_A(b) = A$ leading to

$$\begin{aligned} \frac{\sigma_4(x'_1, x'_2, x_1, x_2)}{d\hat{t}_1 d\hat{t}_2} &= \sigma_4(NN) \cdot \underbrace{\int T(b) d^2b}_A + \\ &+ \frac{f_p(x'_1, x'_2)}{f_p(x'_1) f_p(x'_2)} \frac{d\sigma_2(x'_1, x_1)}{d\hat{t}_1} \frac{d\sigma_2(x'_2, x_2)}{d\hat{t}_2} \underbrace{\int T^2(b) d^2b}_{\propto A^{4/3}}. \end{aligned} \quad (46)$$

In the mean field approximation for NN scattering we use in this article, the $1 \otimes 2$ contribution is strongly suppressed in pA scattering: $R_{pA}/R_{NN} \approx 1/5$ [25].

We find for the ratio double scattering and single scattering terms:

$$\sigma_2/\sigma_1 = 1.1 \left(\frac{\sigma_{eff}}{15 \text{ mb}} \right) \cdot \left(\frac{A}{40} \right)^{.39} (1 + R_{pp}/5), \quad (47)$$

for $A \geq 40$. Hence for the typical hard kinematics: $\sigma_{eff} \sim 15 \div 20\text{mb}$, $R_{NN} = 0.8$ we find the enhancement of DPS as compared to the impulse approximation result:

$$1 + \sigma_2/\sigma_1 \approx 3.5 \div 4.2. \quad (48)$$

for the lead nucleus. Note that Eq. 46 is valid for fixed b as well. Hence we expect that for collisions with heavy nuclei at small b the ratio σ_2/σ_1 is enhanced by an additional factor of ~ 1.5 . Hence one can look for the effect of MPI in pA scattering by comparing central and peripheral pA collisions.

Much larger enhancement is expected for higher order MPI [24]. However only chance to observe such rare events would be for rather small p_{\perp} and small x_A where leading twist shadowing effects would significantly reduce elementary cross sections.

VIII. SOFT – HARD INTERPLAY IN pp COLLISIONS AT THE LHC

A. Underlying event and transverse geometry

The pp LHC data already provide important tests of the transverse geometry of pp collisions described in Sect.II.

Let us first consider production of a hadron (minijet) with momentum p_{\perp} . The observable of interest here is the transverse multiplicity, defined as the multiplicity of particles with transverse momenta in a certain angular region perpendicular to the transverse momentum of the trigger particle or jet (the standard choice is the interval $60^{\circ} < |\Delta\phi| < 120^{\circ}$ relative to the jet axis; see Ref. [62] for an illustration and discussion of the experimental definition). In the central collisions one expects a much larger transverse multiplicity due to the presence of multiple hard and soft interactions. At the same time the enhancement should be a weak function of p_{\perp} in the region where main contribution is given by the hard mechanism [51, 52]. The predicted increase and eventual flattening of the transverse multiplicity agrees well with the pattern observed in the existing data. At $\sqrt{s} = 0.9\text{ TeV}$ the transition occurs approximately at $p_{T,\text{crit}} \approx 4\text{ GeV}$, at $\sqrt{s} = 1.8\text{ TeV}$ at $p_{T,\text{crit}} \approx 5\text{ GeV}$, and at $p_{T,\text{crit}} = 6 - 8\text{ GeV}$ for 7 TeV [63, 64]. Note also that $p_{T,\text{crit}}$ is smaller for the single hadron trigger than for a jet trigger since the leading hadron carries a fraction $\sim 0.6 \div 0.7$ of the jet momentum, see comparison the CMS jet data and ALICE single hadron data in Fig. 3 of [65].

One possible interpretation is the minimum p_{\perp} at which particle production due to hard collisions starts to dominate significantly increases with the collision energy. Another is that for the small p_{\perp} one selects events with fewer DMS collisions due to cutoff on minimum p_{\perp} which becomes stronger with increase of the incident energy. Both these effects are likely to be related the onset of the high gluon density regime in the central pp interactions since with an increase of incident energy leads to partons in the central pp collisions propagating through stronger and stronger gluon fields.

Many further tests of the discussed picture were suggested in Ref. [52]. They include (i) Check that the transverse multiplicity does not depend on rapidities of the jets, (ii) Study of the multi-

plicity at $y < 0$ for events with jets at $y_1 \sim y_2 \sim 2$. This would allow to check that the transverse multiplicity is universal and that multiplicity in the away and the towards regions is similar to the transverse multiplicity for $y \leq 0$. (iii) Studying whether transverse multiplicity is the same for quark and gluon induced jets. Since the gluon radiation for production of W^\pm, Z is smaller than for the gluon dijets, a subtraction of the radiation effect mentioned below is very important for such comparisons.

Note that the contribution of the jet fragmentation to the transverse cone as defined in the experimental analyses is small but not negligible especially at smaller energies ($\sqrt{s} = 0.9\text{TeV}$). It would be desirable to use a more narrow transverse cone, or subtract the contribution of the jets fragmentation. Indeed, the color flow contribution [66] leads to a small residual increase of the transverse multiplicity with p_\perp . However the jet fragmentation effect depends on p_T rather than on \sqrt{s} . Hence it does not contribute to the growth of the transverse multiplicity, which is a factor of ~ 2 between $\sqrt{s} = 0.9\text{TeV}$ and $\sqrt{s} = 7.0\text{TeV}$. In fact, a subtraction of the jet fragmentation contribution would somewhat increase the rate of the increase of the transverse multiplicity in the discussed energy interval. This allows to obtain the lower limit for the rate of the increase of the multiplicity in the central ($\langle b \rangle \sim 0.6\text{ fm}$) pp collisions of $s^{0.17}$. It is a bit faster than the s dependence of multiplicity in the central heavy ion collisions.

B. Correlation of soft and hard multiplicities

It was demonstrate recently [65] that the rates of different hard processes observed in jet production by CMS and in J/ψ , D-meson production by ALICE normalized to the average hard process multiplicity, R universally depend on the underlying event charged-particle multiplicity normalized to the average charged-particle multiplicity at least until it becomes four times higher than average. Note here that the recoil jet multiplicity has to be subtracted from the underlying multiplicity.

It is worth emphasizing here, that similarity between R in the CMS and ALICE measurements is highly non-trivial as the rapidity intervals used for determination of N_{ch} differ by a factor of ~ 3 .

The ratio of the inclusive rate of hard signals at fixed b to the average one in bulk events is given as follows [67]

$$R(b) = P_2(b)\sigma_{inel}. \quad (49)$$

The median of the distribution over N_{ch} should roughly correspond to the median of the distribution

over impact parameters. For the studied inelastic sample $\sigma_{inel} \approx 55$ mb. Using parametrization of P_{2b} from the Appendix we find $R_{median} \approx 2$ which agrees well with the data.

The relation Eq. 49 breaks down when the multiplicity selection starts to select $b \sim 0$ corresponding to $R(0) \approx 4$.

For $b \sim 0$ the trigger on high multiplicity starts to select configurations in colliding nucleons with larger than average number of hard collisions, corresponding to $R(0)$.

In this limit large fraction of the total multiplicity originates from gluon emission in processes associated with minijet production. So one can expect that in this limit $N_{ch}/\langle N_{ch} \rangle$ is proportional to the number of the hard collisions, N , and leading to the linear dependence between N and $N_{ch}/\langle N_{ch} \rangle$. This expectation is consistent with the data.

An interesting question is whether high multiplicity events originate from tail of distribution over number of hard collisions at $b \sim 0$ or from some correlated configurations. In [67] it was suggested that for the highest observed multiplicities (which occur with probability $\sim 10^{-4} \div 10^{-5}$ fluctuations of the gluon density are important.

C. Unitarity and consistency in multiple hard collisions

One of the important observations of the MC models is that to reproduce the data one needs to suppress production of minijets. PYTHIA [46] introduces the energy dependent suppression factor

$$R(p_{\perp}) = p_T^4 / (p_{\perp}^2 + p_0^2(s))^2, \quad (50)$$

with $p_0(\sqrt{s} = 7TeV) \approx 3GeV/c$, corresponding to $R(p_T = 4GeV/c) = 0.4$. In HERWIG [49] a cutoff of similar magnitude is introduced of the form $\theta(p_{\perp} - p'_0(s))$.

A complimentary way to see that a mechanism of the suppression has to exist follows from the analysis of the restrictions related to the value of the total inelastic cross section at a fixed impact parameter [69, 70]. (Note here that the large inclusive cross section of production of minijets which exceeds the total inelastic cross section does not violate the S -channel unitarity since it effectively measures multiplicity of minijet production.)

It is possible to rewrite the cross section of the production of minijets as a series of positive terms $\sigma_i = \int d^2b P f_i(b)$, where $P f_i(b)$ is the probability that in the collision at fixed b exactly i minijet pairs are produced. The total probability of inelastic interaction at given b is expressed through the elastic scattering amplitude (Eq. 8).

Unitarity in the b space leads to the condition

$$P_{hard}(b) = \sum_{i=1}^{\infty} P f_i(b) \leq P_{in}(s, b). \quad (51)$$

As we discussed in section II distribution over b for generic inelastic collisions is much broader than for hard binary collisions and that of binary collisions is much broader than of MPI events (Fig. 2). As a result in a MPI model without nonperturbative correlations one finds that for $b \geq 1.2$ fm inclusive cross section for production of minijets at given b and $P_{hard}(b)$ practically coincide and hence the analysis does not depend on the details of modeling.

Numerical studies indicate that to satisfy inequality Eq. 51 one needs to suppress production of minijets in the momentum range similar to that introduced in the Pythia [46] and HERWIG [49] models.

In fact one may need an even stronger cutoff. Indeed in Eq.51 we did not take into account that inelastic diffraction contributes a significant fraction, $\sim 15 \div 20\%$, of σ_{in} at the LHC and it is predominantly due to events with no minijet production (remember that even in DIS where absorptive effects are small diffraction constitutes a small fraction of the small x cross section ($\leq 20\%$). Since for small b interaction is essentially black and hence diffraction is impossible, the main contribution of diffraction to P_{in} should concentrate at $b \geq 1.2$ fm, leading to a need for even stronger cutoff.

A dynamical mechanism for a strong cutoff for the interaction at large impact parameters is not clear. Indeed, typical x_1, x_2 for hard collisions are $10^{-2} \div 10^{-3}$ for which pQCD work well at HERA. Also, colliding partons of the nucleon "1" ("2") propagate typically through much smaller gluon densities of the the nucleon "2" ("1") so one would expect a very strong dependence of the cutoff on impact parameter. Alternatively, one would have to introduce very strong correlations for partons at the nucleon periphery.

Understanding the origin of this phenomenon is one of the challenges for the future studies.

IX. CONCLUSIONS

We developed the momentum space technique for describing MPI based on introduction of double parton (triple ...) GPDs. It allows effectively introduce both the mean field approximation which is constrained by the data on single parton GPDs and developed the framework for including perturbative and nonperturbative correlations between the partons. We find that perturbative correlations enhance the high p_{\perp} DPS rates bringing into a fair agreement with most of the ex-

periments. In the underlying event kinematics an additional NP mechanism becomes significant which strength was estimated based on information about double Pomeron exchange. NP mechanism largely compensates the increase of σ_{eff} expected in the mean field approximation due to the increase of the gluon distribution radius with decrease of x .

Taken together these three mechanisms provide a good description of experimental data on MPI in the entire kinematical domain, including forward heavy flavor production observed in LHCb [36].

The dijet production and even more so MPI occur at smaller impact parameters than the soft interactions giving leading to explanation of some of regularities of UE and to a conclusion that a strong suppression of minijet production even in peripheral collisions is necessary for explaining pp data.

Further studies are necessary in order to go beyond the leading log approximation as well as to understand dynamical mechanism of the suppression of the minijet production. It would be desirable to find a way to distinguish the scenario presented here with a low Q^2 scale starting point of the pQCD evolution and weak NP correlations at $x > 10^{-3}$ and a scenario where the NP correlations are present at $x \sim 10^{-2}$ while pQCD evolution starts at significantly higher scale.

Next, further work may be needed to describe recent experimental data on J/Ψ production in central kinematics [75, 76].

Here we focused on $x_i < 0.1$ domain. Large x region is certainly of much interest for understanding the nucleon structure. For example, strong quarkantiquark correlations may arise [71] from dynamical chiral symmetry breaking. Also, one expects significant correlations between valence quarks. They could be studied in the forward DPS for example in the production of two forward pions [72].

Acknowledgements

We thank our coauthors M.Azarkin, Yu.Dokshitzer, L. Frankfurt, P. Gunnellini, T. Rogers, A. Stasto, D.Treleani, C. Weiss, U. Wiedemann for numerous discussions and insights. We thank V.Belyaev for discussions of the LHCb charm data. M.S.'s research was supported by the US Department of Energy Office of Science, Office of Nuclear Physics under Award No. DE-FG02-93ER40771.

Appendix

The QCD factorization theorem for exclusive vector meson (VM) production[73] states that in the leading twist approximation the differential cross section of the process $\gamma_L^* + p \rightarrow VM + p$ is given by the convolution of the hard block, meson wave function and generalized gluon parton distribution, $g(x_1, x_2, t | Q^2)$, where x_1, x_2 are the longitudinal momentum fractions of the emitted and absorbed gluon (we discuss here only the case of small x which is of relevance for the LHC kinematics). Of particular interest is the generalized parton distribution (GPD) in the “diagonal” case, $g(x, t | Q^2)$, where $x_1 = x_2$ and denoted by x , and the momentum transfer to the nucleon is in the transverse direction, with $t = -\Delta_\perp^2$ (we follow the notation of Refs. [51, 52]). This function reduces to the usual gluon density in the nucleon in the limit of zero momentum transfer, $g(x, t = 0 | Q^2) = g(x | Q^2)$. Its two-dimensional Fourier transform

$$g(x, \rho | Q^2) \equiv \int \frac{d^2 \Delta_\perp}{(2\pi)^2} e^{i(\Delta_\perp \rho)} g(x, t = -\Delta_\perp^2 | Q^2) \quad (52)$$

describes the one-body density of gluons with given x in transverse space, with $\rho \equiv |\boldsymbol{\rho}|$ measuring the distance from the transverse center-of-momentum of the nucleon, and is normalized such that $\int d^2 \rho g(x, \rho | Q^2) = g(x | Q^2)$. It is convenient to separate the information on the total density of gluons from their spatial distribution and parametrize the GPD in the form

$$g(x, t | Q^2) = g(x | Q^2) F_{2g}(x, t | Q^2), \quad (53)$$

where the latter function satisfies $F_{2g}(x, t = 0 | Q^2) = 1$ and is known as the two-gluon form factor of the nucleon. Its Fourier transform describes the normalized spatial distribution of gluons with given x ,

$$F_{2g}(x, \rho | Q^2) \equiv \int \frac{d^2 \Delta_\perp}{(2\pi)^2} e^{i(\Delta_\perp \rho)} F_{2g}(x, t = -\Delta_\perp^2 | Q^2), \quad (54)$$

with $\int d^2 \rho F_{2g}(x, \rho | Q^2) = 1$ for any x .

The QCD factorization theorem predicts that the t -dependence of the VM production should be a universal function of t for fixed x (up to small DGLAP evolution effects). Indeed the t -slope of the J/ψ production is practically Q^2 independent, while the t -slope of the production light vector mesons approaches that of J/ψ for large Q^2 . The t -dependence of the measured differential cross sections of exclusive processes at $|t| < 1 \text{ GeV}^2$ is commonly described either by an exponential, or by a dipole form inspired by analogy with the nucleon elastic form factors. Correspondingly, we

consider here two parametrizations of the two-gluon form factor:

$$F_{2g}(x, t|Q^2) = \begin{cases} \exp(B_g t/2), \\ (1 - t/m_g^2)^{-2}, \end{cases} \quad (55)$$

where the parameters B_g and m_g are functions of x and Q^2 . The two parametrizations give very similar results if the functions are matched at $|t| = 0.5 \text{ GeV}^2$, where they are best constrained by present data (see Fig. 3 of Ref. [74]); this corresponds to [52]

$$B_g = 3.24/m_g^2. \quad (56)$$

The analysis of the HERA exclusive data leads to

$$B_g(x) = B_{g0} + 2\alpha'_g \ln(x_0/x), \quad (57)$$

where $x_0 = 0.0012$, $B_{g0} = 4.1 \text{ }^{(+0.3)}_{(-0.5)} \text{ GeV}^{-2}$, $\alpha'_g = 0.140 \text{ }^{(+0.08)}_{(-0.08)} \text{ GeV}^{-2}$ for $Q_0^2 \sim 3 \text{ GeV}^2$. For fixed x , $B(x, Q^2)$ slowly decreases with increase of Q^2 due to the DGLAP evolution [51]. The uncertainties in parentheses represent a rough estimate based on the range of values spanned by the H1 and ZEUS fits, with statistical and systematic uncertainties added linearly. This estimate does not include possible contributions to α'_g due to the contribution of the large size configurations in the vector mesons and changes in the evolution equation at $-t$ comparable to the intrinsic scale. Correcting for these effects may lead to a reduction of α'_g and hence to a slower increase of the area occupied by gluons with decrease of x .

-
- [1] T. Sjostrand and M. van Zijl, Phys. Rev. D **36** (1987) 2019.
- [2] A. Grebenyuk, F. Hautmann, H. Jung, P. Katsas and A. Knutsson, Phys. Rev. D **86** (2012) 117501 [arXiv:1209.6265 [hep-ph]]
- [3] N. Paver and D. Treleani, Nuovo Cim. A **70** (1982) 215.
- [4] M. Mekhfi, Phys. Rev. D **32**, 2371 (1985).
- [5] J.R. Gaunt and W.J. Stirling, JHEP **1003**, 005 (2010) [arXiv:0910.4347 [hep-ph]];
- J.R. Gaunt, C.H. Kom, A. Kulesza and W.J. Stirling, Eur. Phys. J. C **69**, 53 (2010) [arXiv:1003.3953 [hep-ph]].
- [6] B. Blok, Yu. Dokshitzer, L. Frankfurt and M. Strikman, Phys. Rev. D **83**, 071501 (2011) [arXiv:1009.2714 [hep-ph]].
- [7] M. Diehl, PoS D **IS2010** (2010) 223 [arXiv:1007.5477 [hep-ph]].

- [8] J.R. Gaunt and W.J. Stirling, JHEP **1106**, 048 (2011) [arXiv:1103.1888 [hep-ph]].
- [9] B. Blok, Yu. Dokshitzer, L. Frankfurt and M. Strikman, Eur. Phys. J. C **72**, 1963 (2012) [arXiv:1106.5533 [hep-ph]].
- [10] M. Diehl, D. Ostermeier and A. Schafer, JHEP **1203** (2012) 089 [arXiv:1111.0910 [hep-ph]].
- [11] B. Blok, Yu. Dokshitzer, L. Frankfurt and M. Strikman, arXiv:1206.5594v1 [hep-ph] (unpublished).
- [12] B. Blok, Y. Dokshitzer, L. Frankfurt and M. Strikman, Eur. Phys. J. C **74** (2014) 2926 [arXiv:1306.3763 [hep-ph]].
- [13] A. V. Manohar and W. J. Waalewijn, Phys. Lett. B **713** (2012) 196 [arXiv:1202.5034 [hep-ph]].
- [14] A. V. Manohar and W. J. Waalewijn, Phys. Rev. D **85** (2012) 114009 [arXiv:1202.3794 [hep-ph]].
- [15] J. R. Gaunt, R. Maciula and A. Szczurek, Phys. Rev. D **90** (2014) no.5, 054017 [arXiv:1407.5821 [hep-ph]]. arXiv:1407.5821 [hep-ph].
- [16] K. Golec-Biernat and E. Lewandowska, Phys. Rev. D **90** (2014) no.9, 094032 [arXiv:1407.4038 [hep-ph]].
- [17] M. Diehl, J. R. Gaunt, D. Ostermeier, P. Pobl and A. Schafer, JHEP **1601** (2016) 076 [arXiv:1510.08696 [hep-ph]].
- [18] J. R. Gaunt, JHEP **1301** (2013) 042 doi:10.1007/JHEP01(2013)042 [arXiv:1207.0480 [hep-ph]].
- [19] R. Astalos *et al.*, “Proceedings of the Sixth International Workshop on Multiple Partonic Interactions at the Large Hadron Collider,” arXiv:1506.05829 [hep-ph].
- [20] ‘Proceedings of the Seventh International Workshop on Multiple Partonic Interactions at the Large Hadron Collider,’
- [21] B. Blok and P. Gunnellini, Eur. Phys. J. C **75** (2015) no.6, 282 [arXiv:1503.08246 [hep-ph]].
- [22] B. Blok and P. Gunnellini, Eur. Phys. J. C **76** (2016) no.4, 202 [arXiv:1510.07436 [hep-ph]].
- [23] B. Blok and M. Strikman, Eur. Phys. J. C **74** (2014) 3038 [arXiv:1402.5374 [hep-ph]].
- [24] M. Strikman and D. Treleani, Phys. Rev. Lett. **88**, 031801 (2002) doi:10.1103/PhysRevLett.88.031801 [hep-ph/0111468].
- [25] B. Blok, M. Strikman and U. A. Wiedemann, Eur. Phys. J. C **73** (2013) no.6, 2433 [arXiv:1210.1477 [hep-ph]].
- [26] B. Blok and M. Strikman, Eur. Phys. J. C **74** (2014) no.12, 3214 [arXiv:1410.5064 [hep-ph]].
- [27] B. Blok and M. Strikman, Eur. Phys. J. C **76** (2016) no.12, 694 [arXiv:1608.00014 [hep-ph]].
- [28] B. Blok and M. Strikman, Phys. Lett. B **772** (2017) 219 [arXiv:1611.03649 [hep-ph]].
- [29] F. Abe *et al.* [CDF Collaboration], Phys. Rev. D **56**, 3811 (1997).
- [30] V.M. Abazov *et al.* [D0 Collaboration], Phys. Rev. D **81**, 052012 (2010).
- [31] V.M. Abazov *et al.* [D0 Collaboration], Phys. Rev. D **83**, 052008 (2011).
- [32] S. Chatrchyan *et al.* [CMS Collaboration], Phys. Rev. D **89** (2014) 9, 092010 [arXiv:1312.6440 [hep-ex]].
- [33] G. Aad *et al.* [ATLAS Collaboration], Phys. Rev. D **83** (2011) 112001 [arXiv:1012.0791 [hep-ex]].
- [34] G. Aad *et al.* [ATLAS Collaboration], New J. Phys. **15**, 033038 (2013) doi:10.1088/1367-2630/15/3/033038 [arXiv:1301.6872 [hep-ex]].
- [35] S. Chatrchyan *et al.* [CMS Collaboration], JHEP **1403** (2014) 032 [arXiv:1312.5729 [hep-ex]].

- [36] I.M. Belyaev, talk at MPI-2015 conference.
- [37] R. Aaij et al. (LHCb collaboration), JHEP, 1206(2012), 141,1403 (2014)108 arXiv: 1205.0975v3.
- [38] R. Aaij et al (LHCb collaboration), Nucl. Phys. B871 (2013) 1.
- [39] R. Aaij et al (LHCb collaboration), arXiv: 1510.05949 Phys. Rev. D **36** (1987) 2019.
- [40] J. M. Butterworth, J. R. Forshaw and M. H. Seymour, Z. Phys. C **72** (1996) 637 [hep-ph/9601371].
- [41] T. Sjostrand and P. Z. Skands, Eur. Phys. J. C **39** (2005) 129 [hep-ph/0408302].
- [42] S. Gieseke, C. A. Rohr and A. Siodmok, arXiv:1110.2675 [hep-ph]; S. Gieseke, D. Grellscheid, K. Hamilton, A. Papaefstathiou, S. Platzer, P. Richardson, C. A. Rohr and P. Ruzicka *et al.*, arXiv:1102.1672 [hep-ph].
- [43] M. H. Seymour and A. Siodmok, JHEP **1310** (2013) 113 [arXiv:1307.5015 [hep-ph]].
- [44] S. Gieseke, C. Rohr and A. Siodmok, Eur. Phys. J. C **72** (2012) 2225 [arXiv:1206.0041 [hep-ph]].
- [45] M. Bähr, M. Myska, M.H. Seymour and A. Siodmok, arXiv: 1302.4325 [hep-ph]
- [46] T. Sjostrand *et al.*, Comput. Phys. Commun. **191** (2015) 159 doi:10.1016/j.cpc.2015.01.024 [arXiv:1410.3012 [hep-ph]].
- [47] R. Corke and T. Sjöstrand, JHEP **1105** (2011) 009 [arXiv:1101.5953 [hep-ph]].
- [48] R. Corke and T. Sjöstrand, JHEP **1103** (2011) 032 [arXiv:1011.1759 [hep-ph]].
- [49] J. M. Butterworth, J. R. Forshaw and M. H. Seymour, Z. Phys. C **72** (1996) 637 [hep-ph/9601371].
- [50] C. Flensburg, G. Gustafson, L. Lonnblad and A. Ster, arXiv:1103.4320 [hep-ph].
- [51] L. Frankfurt, M. Strikman and C. Weiss, Phys. Rev. D **69**, 114010 (2004) [arXiv:hep-ph/0311231],
L. Frankfurt, M. Strikman and C. Weiss, Ann. Rev. Nucl. Part. Sci. **55**, 403 (2005) [arXiv:hep-ph/0507286].
- [52] L. Frankfurt, M. Strikman and C. Weiss, Phys. Rev. D **83**, 054012 (2011) doi:10.1103/PhysRevD.83.054012 [arXiv:1009.2559 [hep-ph]].
- [53] M. Strikman, Acta Phys. Polon. B **42**, 2607 (2011) doi:10.5506/APhysPolB.42.2607 [arXiv:1112.3834 [hep-ph]].
- [54] D. d’Enterria and A. M. Snigirev, Phys. Rev. Lett. **118** (2017) no.12, 122001 [arXiv:1612.05582 [hep-ph]].
- [55] Y. L. Dokshitzer, D. Diakonov and S. I. Troian, Phys. Rept. **58**, 269 (1980).
- [56] M. Gluck, E. Reya and A. Vogt, Z. Phys. C **53** (1992) 127.
- [57] C. Adloff *et al.* [H1 Collaboration], Z. Phys. C **74** (1997) 221 [hep-ex/9702003].
- [58] E. G. S. Luna, V. A. Khoze, A. D. Martin and M. G. Ryskin, Eur. Phys. J. C **59** (2009) 1 [arXiv:0807.4115 [hep-ph]]
- [59] M. Gluck, E. Reya and A. Vogt, Eur. Phys. J. C **5** (1998) 461 [hep-ph/9806404].
- [60] F. D. Aaronson *et al.*[H1 Collaboration], JHEP 1005, 032 (2010)
- [61] B. Blok and M. Strikman, Eur. Phys. J. C **74**, 3038 (2014) doi:10.1140/epjc/s10052-014-3038-5 [arXiv:1402.5374 [hep-ph]].
- [62] T. Affolder *et al.* [CDF Collaboration], Phys. Rev. D **65**, 092002 (2002).

- doi:10.1103/PhysRevD.65.092002
- [63] S. Chatrchyan *et al.* [CMS Collaboration], JHEP **1109** (2011) 109 doi:10.1007/JHEP09(2011)109 [arXiv:1107.0330 [hep-ex]].
- [64] G. Aad *et al.* [ATLAS Collaboration], Eur. Phys. J. C **71** (2011) 1636 doi:10.1140/epjc/s10052-011-1636-z [arXiv:1103.1816 [hep-ex]].
- [65] M. Y. Azarkin, I. M. Dremin and M. Strikman, Phys. Lett. B **735** (2014) 244 [arXiv:1401.1973 [hep-ph]].
- [66] Y. L. Dokshitzer, V. A. Khoze, A. H. Mueller and S. I. Troian, Gif-sur-Yvette, France: Ed. Frontieres (1991) 274 p.
- [67] M. Strikman, Phys. Rev. D **84**, 011501 (2011) doi:10.1103/PhysRevD.84.011501 [arXiv:1105.2285 [hep-ph]].
- [68] T. C. Rogers, A. M. Stasto and M. I. Strikman, Phys. Rev. D **77**, 114009 (2008) [arXiv:0801.0303 [hep-ph]].
- [69] T. C. Rogers, A. M. Stasto and M. I. Strikman, Phys. Rev. D **77**, 114009 (2008) doi:10.1103/PhysRevD.77.114009 [arXiv:0801.0303 [hep-ph]].
- [70] T. C. Rogers and M. Strikman, Phys. Rev. D **81**, 016013 (2010) [arXiv:0908.0251 [hep-ph]].
- [71] P. Schweitzer, M. Strikman and C. Weiss, JHEP **1301**, 163 (2013) doi:10.1007/JHEP01(2013)163 [arXiv:1210.1267 [hep-ph]].
- [72] M. Strikman and W. Vogelsang, Phys. Rev. D **83**, 034029 (2011) doi:10.1103/PhysRevD.83.034029 [arXiv:1009.6123 [hep-ph]].
- [73] J. C. Collins, L. Frankfurt and M. Strikman, Phys. Rev. D **56** (1997) 2982 doi:10.1103/PhysRevD.56.2982 [hep-ph/9611433].
- [74] L. Frankfurt, C. E. Hyde, M. Strikman and C. Weiss, Phys. Rev. D **75** (2007) 054009 doi:10.1103/PhysRevD.75.054009 [hep-ph/0608271].
- [75] V. Khachatryan *et al.* [CMS Collaboration], JHEP **1409** (2014) 094 doi:10.1007/JHEP09(2014)094 [arXiv:1406.0484 [hep-ex]].
- [76] J. P. Lansberg, H. S. Shao and N. Yamanaka, arXiv:1707.04350; J. P. Lansberg and H. S. Shao, JHEP **1610** (2016) 153 doi:10.1007/JHEP10(2016)153 [arXiv:1608.03198; J. P. Lansberg and H. S. Shao, Nucl. Phys. B **900** (2015) 273 doi:10.1016/j.nuclphysb.2015.09.005 [arXiv:1504.06531 [hep-ph]].